ASSOCIATION EURATOM - UNIVERSITY OF LATVIA

AEUL

ANNUAL REPORT 2011

Riga 2012

TABLE OF CONTENT

1. INTRODUCTION

This Annual Report summarises the fusion research activities of the Latvian Research Unit of the Association EURATOM-University of Latvia in 2011.

There is now general agreement that the economy of the world must be radically transformed in the coming decades, either because fossil fuels become exhausted, or because of environmental concerns relating to emission of CO_2 and other greenhouse gases. In this context, fusion power may come to play a critical role in meeting the energy requirements of the world.

Fusion energy is a safe form of nuclear energy, which does not pollute the atmosphere. The fundamental "fuels" heavy hydrogen (deuterium) and lithium are found abundantly in seawater and in the earth's crust and will provide the world with energy in the many millions of years. The primary waste is the power plant. Power plants become radioactive, but the radioactivity will be gone after 100 years, and there will therefore be no need for long-term storage of waste.

Worldwide coordinated fusion research started in the late 1950s to find ways to use fusion as an energy source here on Earth. In 2006 seven parties, EU, Japan, Russia, China, USA, Korea and India, signed the agreement to build and exploit ITER - International Thermonuclear Experimental Reactor, and to place ITER in Cadarache in France. It is expected that ITER will be ready for scientific exploitation in 2024.

The mission of ITER is to demonstrate that nuclear fusion can be exploited as an energy source. ITER represents an unexpected international cooperation in the field of science and technology. ITER also represents a valuable opportunity for cooperation between public research organisations and private industry.

The principle being pursued with ITER is the fusion of hydrogen isotopes (deuterium and tritium) to form helium. To make the fusion process run at significant rate the hydrogen gas must be heated to high temperatures where it ionises and turns into a plasma. The plasma must be confined to achieve suitable densities and sustain the high temperature. ITER will use a magnetic field for the confinement.

After ITER a prototype commercial power station DEMO will be constructed. DEMO is expected to be operational sometime in the 2030s, so that widespread adoption could occur in mid-century.

In 2011we observed a 10th anniversary of the Association EURATOM-University of Latvia (AEUL). A festive conference was organized January 17, 2012. Speeches were delivered by State Secretary of Latvian Ministry of Education and Sciences Mrs. Lauma Sika, by Rector of University of Latvia Marcis Auzins, by President of Latvian Academy of Sciences Juris Ekmanis, by HRU of AEUL Andris Sternberg.

E-mailed greetings we got from our recent EURATOM Steering Committee members Vito Marchese, Marc Pipeleers and Marc Cosyns as well as from Yvan Capouet.

The activities of the Research Unit are continued in fusion science and technology under the Contract of Association and Technology Programme under EFDA.
The AEUL in the frame of the EFDA Workprogramme 2008 starts to take part in the Goal Oriented Training Programme - GOT "EUROBREED".

The Physics Programme is carried out at IP UL – Institute of Physics, University of Latvia, and at ISSP UL – Institute of Solid State Physics, University of Latvia. The research areas of the Physics Programme are:

- Preparation of a gallium jet limiter for testing under reactor relevant conditions
- Characterization of the impurity concentration, profiling and erosion in ITER relevant materials using *ex situ* LIBS spectroscopy
- *In situ* tokamak laser enhanced LIBS spectroscopy of the impurity concentration depth profile in wall tiles.

Theory and Code Development:

- On the theory of high-power gyrotrons with uptapered resonators
- Structure and dynamics of sawteeth crashes in ASDEX Upgrade
- Computer modelling of impurity clusters in steels; HPC facilities are efectively used to perform large-scale calculations of ODS steels.

The Technology Programme is carried at ICP UL - Institute of Chemical Physics, University of Latvia. The technology research and development under EFDA JET is focused on:

- Analysis of tritium distribution in plasma facing components
- Release of tritium from neutron-irradiated pebbles
- Radiolysis of plasma synthesized lithium orthosilicate nanopowders.

Several Staff Mobility actions took place in 2011: to IPP Garching, FZK Karlsruhe, UKAEA Culham, ISTTOK Lisbon, and Meriland University.

Finally I wish to thank all the staff members of AEUL for their contribution and Latvian Ministry of Education and Sciences for continuous support.

Riga, August 2012

(Andris Sternberg, Head of Research Unit of AEUL)

2. FUSION PROGRAMME ORGANISTION

2.1 Programme Objectives

The Latvian Fusion Programme, under the Association EURATOM-University of Latvia, is fully integrated into the European Programme, which has set the long-term aim of the joint creation of prototype reactors for power stations to meet the needs of society: operational safety, environmental compatibility and economic viability. The objectives of the Latvian programme are: (i) to carry out high-level scientific and technological research in the field of nuclear fusion, (ii) to make a valuable and visible contribution to the European Fusion Programme and to the international ITER Project in our focus areas. This can be achieved by close collaboration with other Associations.

2.2 Association EURATOM-University of Latvia (AEUL)

The Latvian contribution to the European fusion programme began in 2000 in the form of cost-sharing actions (fixed contribution contracts with EURATOM). The Association was established on 19 December 2001 incorporating the existing cost-sharing actions into its work plan.

2.3 Fusion Research Units

The Latvian Research Unit of the Association EURATOM-University of Latvia consists of three Institutes of University of Latvia.

1. IP UL – Institute of Physics, University of Latvia
   32 Miera St., Salaspils LV-2169, Latvia.
   Phone +371 6 7944700, Fax. +371 6 7901214
2. ISSP UL – Institute of Solid State Physics, University of Latvia
   8 Kengaraga St., Riga LV-1063, Latvia.
   Phone +371 6 7187810, Fax. +371 6 7132778
3. ICP UL - Institute of Chemical Physics, University of Latvia
   4 Kronvalda Blvd., Riga LV-1010, Latvia.
   Phone +371 6 7033884, Fax. +371 6 7033884

2.4 Association Steering Committee

The research activities of the Latvian Association EURATOM-University of Latvia are directed by the Steering Committee, which comprises the following members in 2008:

Mr. Vito Marchese Scientific Oficer K6

Mr. Rugerio Gianella Scientific Oficer K6

Mr. Marc Pipeleers, Financial Officer K7

Mrs. Irina Arhipova, Ministry of Education and Science

Mr. Ivars Lacis, University of Latvia

Mr. Andrejs Silins, Latvian Academy of Sciences

The Steering Committee had one meeting in 2011. This meeting was organised as video Conference on July 2, 2011 with remote participation of EU Commission representatives.

2.5 The Latvian Members in the EU Fusion Committees

Consultative Committee for the EURATOM Specific Research and Training Programme in the Field of Nuclear Energy-Fusion (CCE-FU)

Mr. Andris Sternberg, ISSP UL

EFDA Steering Committee

Mr. Andris Sternberg, ISSP UL

Governing Board for the Joint European Undertaking for ITER and the Development of Fusion Energy, "Fusion for Energy" (F4E GB)

Mrs. Maija Bundule, Latvian Academy of Sciences

Mr. Andris Sternberg, ISSP UL

EFDA Public Information Group(recently – Public Information Network – PIN)

Mr. Maris Kundzins, ISSP UL

2.6 Public Information

Conferences

Results of fusion research were presented at:

- The annual scientific conference of University of Latvia.
- The 27th and 28th Scientific Conferences of Institute of Solid State Physics, University of Latvia.
- International Conferences "Functional Materials and Nanotechnologies" (FM&NT-2012, FM&NT-2011) Riga, Institute of Solid State Physics, University of Latvia

Educational activities

Excursions at ISSP UL from schools were organized two to three times a month for PhD students from Latvian universities. Booklets about ISSP UL and EFDA were distributed.

Television, press

Presentation in the television broadcasts TV1, TV7, TV24 and interviews in the newspapers "Neatkarīgā rīta avīze" and "Latvijas avīze".

Presentations in Radio – popular science broadcast.

Popularization of science

Presentation in the TV programme "Science in Latvia",

Presentation in the programme "Researchers Night in Latvia" on 26th of September, 2011.

2.7 Funding and Research Volume 2011

In 2011 the expenditure of the Association EURATOM-University of Latvia was:

Item	Expenditure (EUR)
General Support (20% EU contribution)	
Physics	**475 731**
TOTAL	**475 731**
GOT EOROBREED	**19 509**
HYDOBE	**44 895**
Priority Actions (Additional 20% EU contribution)	**16 000**
Missions and Secondments under the Agreement on Staff Mobility (100% EU contribution)	**10 645**

3. PHYSICS PROGRAMME – FUSION PHYSICS

3.1. Addaptation of liquid metal (LM) stands for experiments with LM jets and droplets under high power loads.

WP 11-PWI-04-04/AEUL/BS

Principal investigator: E.Platacis.
Staff members: O.Lielausis, J.Freibergs, A.Klukins, J.Peinbergs, D.Peinbergs, K.Kravalis

3.1.1. A single InGaSn jet in a strong non-homogeneous 2D magnetic field

Liquid metals remain as one of the most promising candidates if protection of plasma facing or other high-loaded components is considered. The first chapter of our report is devoted to a further development of the liquid metal jet/droplet protecting systems. The results gained with liquid gallium jet/droplet limiter on the small size tokamak ISTTOK are confirming the potential of such an approach. These results have been summarized in two 2011 publications, see [1] and [2]. The ISTTOK has been successfully operated without a degradation of the discharge or a significant contamination of the plasma by the liquid metal. It was stated that the power extraction capability of a Ga jet is fully considerable and corresponds to the most optimistic initial expectations. At rather limited parameters (velocity 2.5m/s; diameter 0.23 cm) the jet was able to extract 2.4 kW from the plasma. A definite specific surface load can also been deduced. It leads to a number of the order of 10 MW/m^2, it means, to a fully divertor relevant value. In the same time a definite modification of the jets trajectory was also detected. The reasons of this small (order 0.5cm on a distance of 50 cm) deflection still remain unclear. According to the existing information the influence of the field on a jet is basically stabilizing. However, the corresponding experience has been gained practically only by experiments in homogeneous fields. In the more general case when a jet/droplet stream crosses a complex 2D and 3D magnetic field additional information is needed. First at all, high gradient magnetic fields should be introduced in the experimental praxis. We have done this on our 5T superconducting magnet. The investigation of the distribution of the field must be considered as an important preparatory step in this direction. The dimensions of the magnet and the distribution of the field along the axis can be seen in Fig. 3.1.1. Fig. 3.1.2 illustrates the results of a rough field's computation. In parallel, the distribution of the field was carefully measured. The measured field lines have also been presented, however, for the most important high gradient region only. The result – we are able to draw a detailed picture of the field in any interesting to us position and direction.

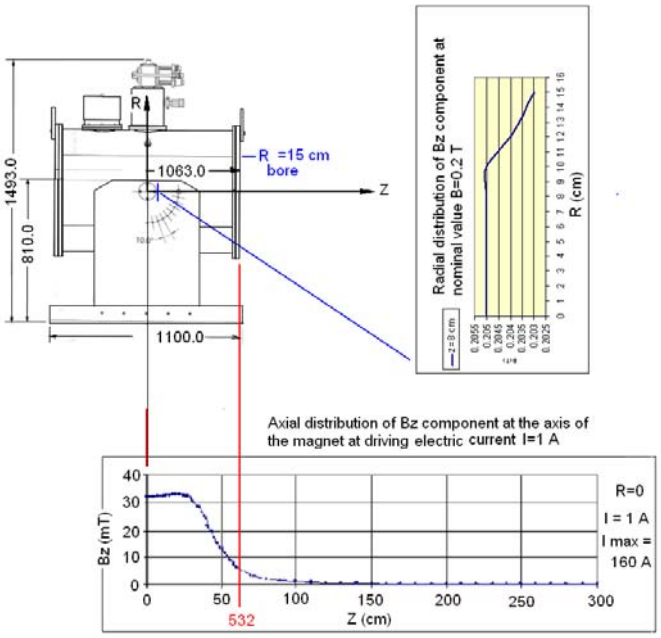

Fig.3.1.1. Scheme of the magnet and the distribution of the field along the axis.

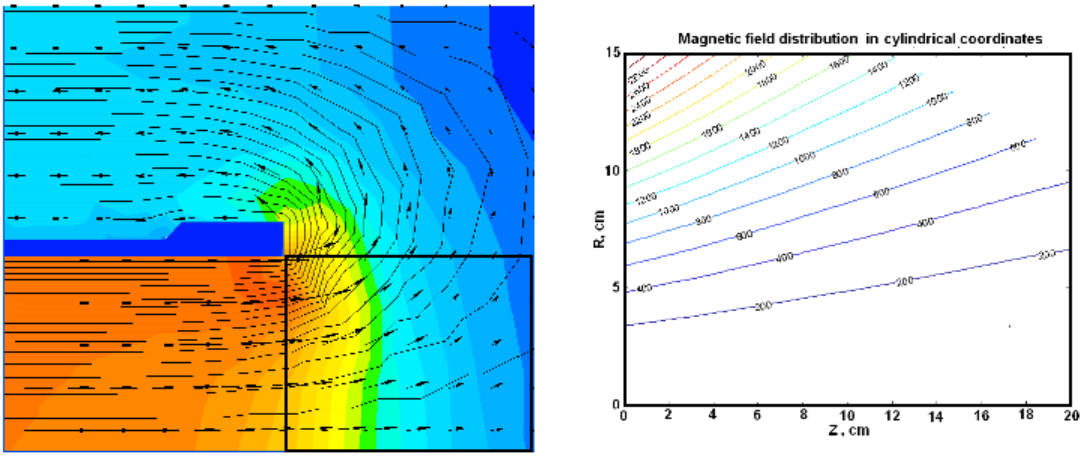

Fig.3.1.2. Computed and measured field lines in the high gradient region.

Let us start the consideration of the latest results with an experiment described already in [2] and presented here in Fig. 3.1.3. To generate a flow of InGaSn the same stand was used which was developed for the preparation of experiments on ISTTOK. The stand was connected to the magnet by a parallel hydraulic branch. The test section was represented by a glass cylinder with openings in the centers of the lid (for

introduction of the nozzle) and in the bottom (for draining). Without the field the jet was behaving like a living thing, with definite fluctuations, etc. Already in a 1T field the jet looked like a string, without any remarkable deflections or splashing.

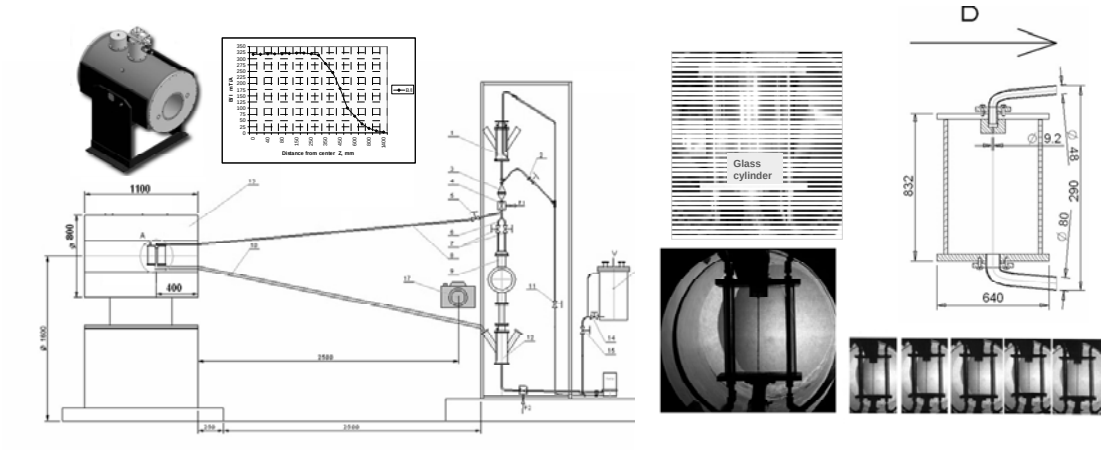

Fig.3.1.3. Stand for investigation of the stability of LM jets in homogeneous fields.

This picture remained unchanged also at the values of the field 2T, 3T, 4T and 5T, as shown in the line of photos. This result serves as a nice additional argument to the statement that, in general, the influence of an orthogonal field on a jet is stabilizing. However, under the already mentioned conditions since the test section was placed in the practically homogeneous part of the field. To introduce into consideration strongly inhomogeneous fields a similar by sense experiment was repeated in configuration presented in Fig. 3.1.4.

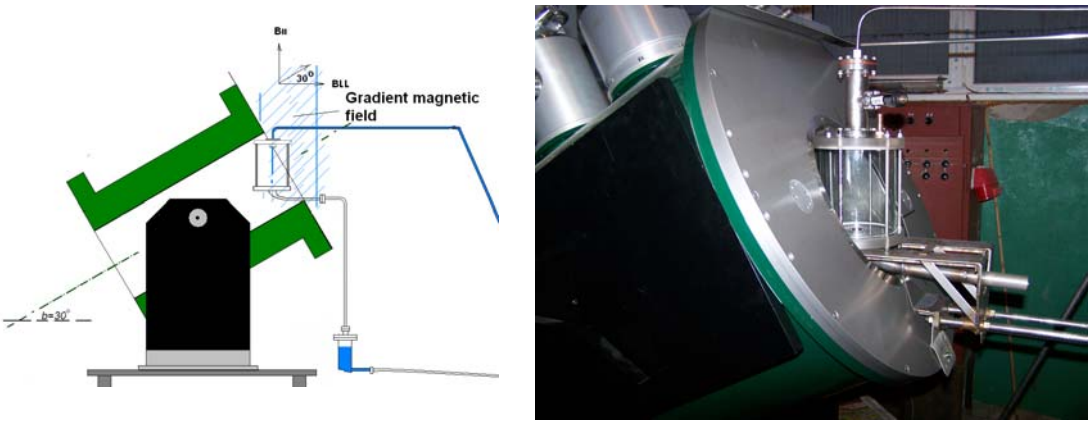

Fig. 3.1.4. Scheme for investigation of LM jets placed in non-homogeneous fields.

Fig. 3.1.5. Installation for investigation of InGaSn jet/droplet streams in non-homogeneous fields.

. The axis of the magnet was turned for 30 degrees. The test section was placed in the inlet part of the solenoid. The installation in general is represented in Fig. 3.1.5. It is shown also that the vertical direction was defined by a laser beam. The main result is represented in Fig.3.1. 6. A jet (d=2.3mm) was directed downward with a velocity of 2.5 m/s. The field in the centre of the magnet was increased from 1T to 4T. In spite of this, the jet continued running strongly parallel to the vertical line which is marked by the laser. The distribution of the magnetic field along the axis of the jet has also been given. In the maximum 4T case the orthogonal to the axis component of the field increases from 1T to 3.5T. This increase is characterized by a practically constant gradient 9.1 T/m. The longitudinal to the axis component decreases from 1.25T to 0T with a mean gradient of the order 1T/m. The gradient of the orthogonal field, equal to 9 T/m, can is considerable indeed. In spite of this, the jet remained practically non-deflected.

According to Fig. 3.1.4 the deflection of the jet should be expected in the “x” direction. The presented in Fig. 3.1.6 photo was taken in the orthogonal “y” direction. However, periodically observations were made also along the “x” axis. The intention was to gain some information about the break-up performances of a jet in a strongly non-uniform field. The break-up in droplets should be expected during the transfer to lower velocities. And indeed, a velocity was fixed, when directly after the nozzle the jet was fully broken-up in droplets. Because of the presence of the field it was difficult to arrange a good enough directional lighting. On the screen of the camera the pictures were acceptably clear. However, after reproduction this quality has been lost and some explanations to the result are needed. In Fig. 3.1.7 the initial picture is presented, and indeed, it is difficult to detect a clear break- up of the jet. In a parallel drawing the individual droplets have been specially marked and the result is clear.

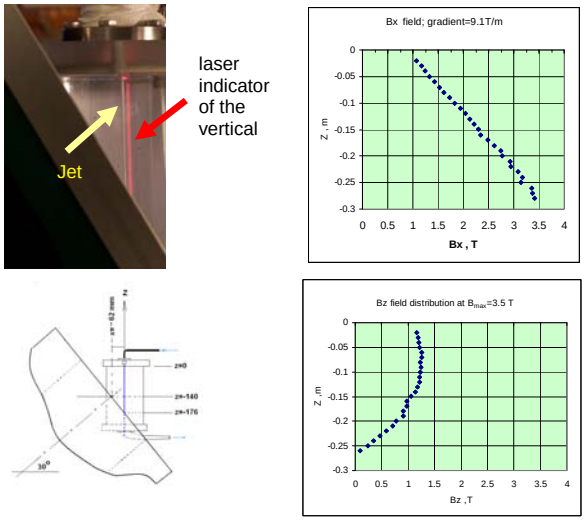

Fig. 3.1.6. The jet in a high-gradient field.

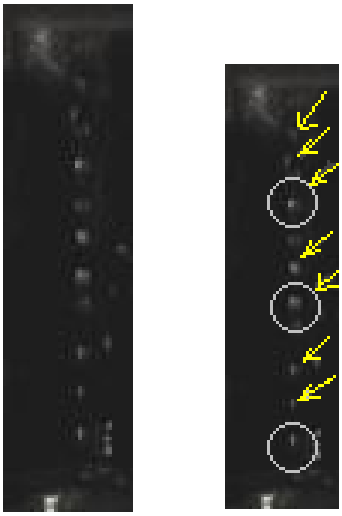

Fig. 3.1.7. Break- up of the jet in droplets.

3.1.2. Behavior of InGaSn jets after touching to a conducting flat plate in the presence of a strong magnetic field.

As mentioned, liquid metals have been considered as potential candidates for the protection of plasma facing components. A plate protected by a fast liquid metal film would represent an ideal version here. However, at such a type of motion the influence of the magnetic field is generally disturbing. As a consequence, CPS systems, systems of jets, droplets, etc. appeared. According to our experience the disturbances in flat free surface MHD flows have been generated mainly by processes typical to the Hartmann walls. A definite role is played also by conditions in the flat inlet nozzle. In our 2010task we started to consider a new version when the liquid metal has been spread over the acting plate by a system of small circular nozzles. Fig. 3.1.8 illustrates the situation when a single InGaSn jet is touching to a SS steel plate under a small angle. The plate is glued on the surface of a permanent magnet which generates an orthogonal to the plate field with the intensity of order of 0.6 T.

Fig. 3.1.8. Spreading of a jet over a conducting plate.

In addition to this, the plate is carefully vetted. In such a way a good electrical contact is ensured. Under such conditions the process of interaction becomes defined by the inertial, by the surface tensional and by the Hartmann forces. It can be seen that after a definite distance the d=2.5 mm jet equally covers the full 3cm width of the breaking plate. It is a result which could be expected.

However, in the case of a divertor the main component of the field is directed tangential to the working plate. To come closer to such conditions the experimental plate was installed in a vacuum tight cylindrical container. The scheme of the plate is shown in Fig. 3.1.9. The container was placed in the inlet part of the mentioned above magnet. The magnet was turned back horizontally.

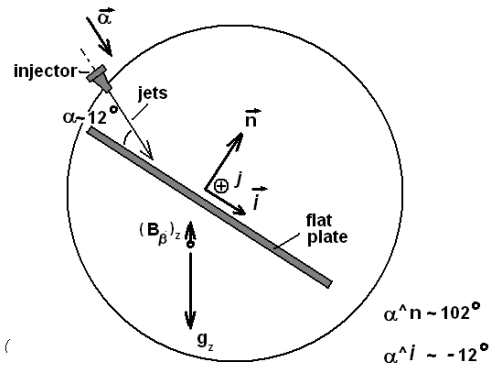

Fig. 3.1.9. Geometry of the experiment.

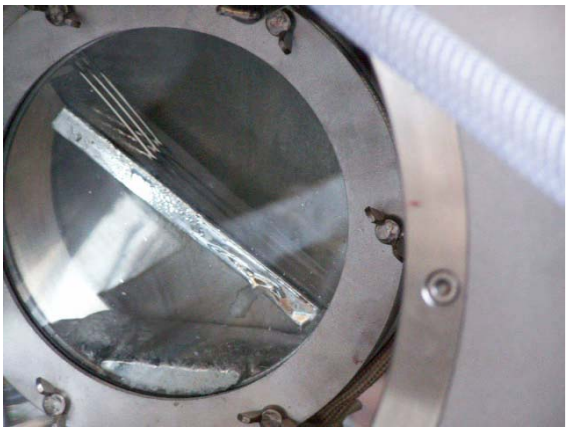

Fig. 3.1.10. Three jets touching with the plate.B= 1T(magn.center); V=2.07 m/s

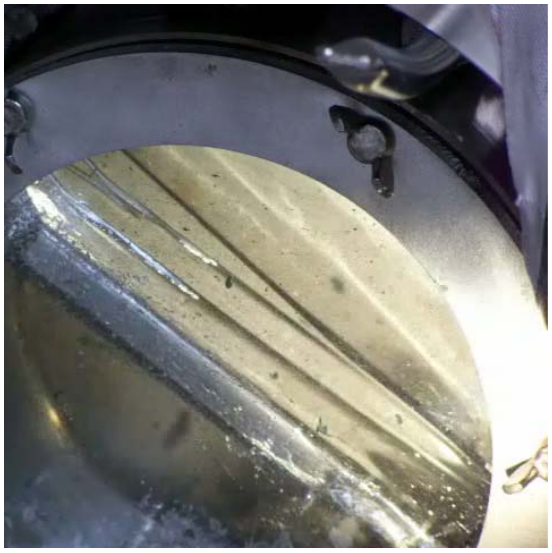

Fig. 3.1.11. Two running in parallel jets B=4T ; V=.27 m/s

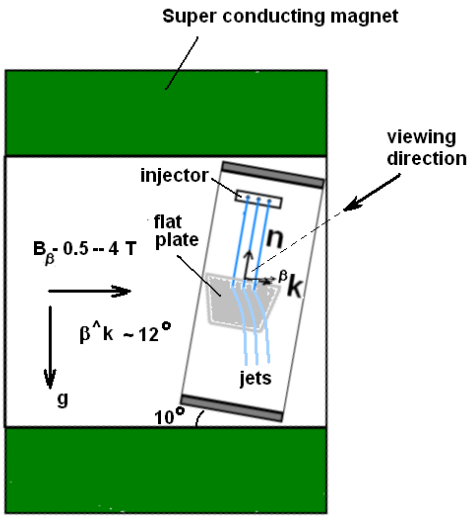

Fig.3.1.12. Graphical illustration of the results.

With regard to the axis of the magnet the container (together with the plate) was turned for 10 degrees. In such a way the typical to divertors topography of the field was approximately reproduced – 90% tangential, 10% orthogonal. The field was clearly non-homogeneous. For more details we must remember on Fig. 3.1.2 where the field's distribution is given. In Fig. 3.1.10 a photo is presented which characterizes the "ideal" initial situation - three parallel jets nicely touching with the plate. The diameter of the nozzles equals to 2.3mm. The number of activated jets can be changed, as well as the velocity in each of the jets. During the experiments the magnetic field was increased up to 4T, the velocities varied in the range from 0.5 m/s t 2.5 m/s. The results must be defined at least as unexpected. So, there were some grounds to expect that the jets will be in one or another way spread over the surface of the plate. Here we can remind on the seemingly similar experiment represented by Fig.8. Under the new conditions the jets clearly tended to a local compactness, instead of spreading. In Fig. 3.1.11 it is shown how two jets remain running practically parallel over the full length of the plate. A similar situation was fixed in a great number of other photos, for one, two or all the three jets. In Fig. 3.1.12 the scheme of the experiment is presented. Basing on Fig. 3.1.11 an additional phenomenon can be introduced in consideration. The jets have been bent/deflected deeper into the magnet, even somewhat uphill, since the plate is inclined for approx.10^0 with regard to the horizon. More in details this effect is shown in Fig. 3.1.13 where the behaviour of a single jet is shown.

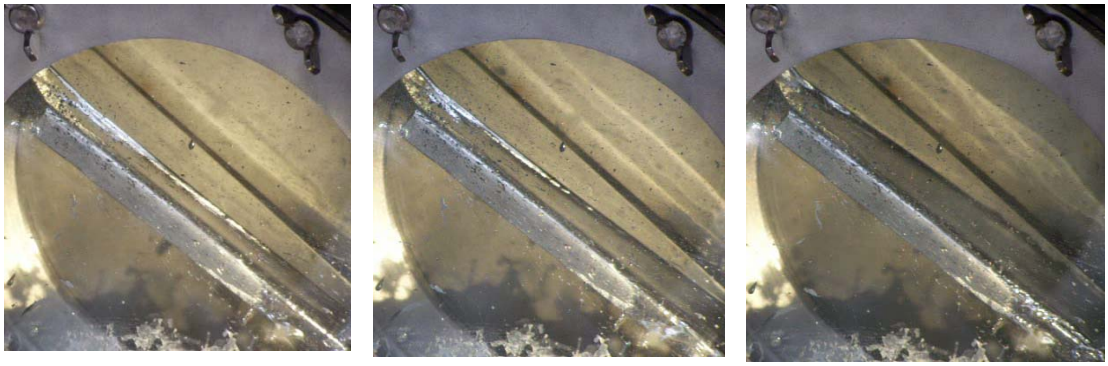

Fig. 3.1.13.The behaviour of a single jet at gradually decreasing velocities: B=4 T; velocity (from left to right):373; 250; 127 cm/s.

Fig. 3.1.14. The behaviour of jets in the case of a quasi-tangential touching with the plate. B=4T

Fig. 3.1.14 corresponds to a new situation when the angle of "attack" was remarkably lowered. The jets were touching with the plate quasi-tangentially. Under definite conditions a specific instability appeared. In a sporadically way the jets

started to lose touch with the plate. For a definite of time they could even remain in a free-flight regime over the full length of the track, from the nozzle till the touching point with the wall of the container.

Attention should be paid to the boundary conditions typical to the described "strange" MHD processes. First, the magnetic field was non-uniform. Second, all the time the liquid metal was in good electrical contact with the metallic components of the experimental container.

References (2011 Publications)

1. R.B.Gomes, C.Silva, H.Fernandes, P.Duarte, I.Nedzelskiy, O.Lielausis, A.Klykin, E. Platacis - " ISSTOK tokamak plasmas influence on a liquid gallium jet dynamic behavior", Journal of nuclear materials 415(2011) S989-S992

2. O. Lielausis, A. Klykin, E. Platacis, A. Mikelsons, R.B. Gomes, H. Fernandes, C. Silva "Stability of liquid metal jet in the context of fusion applications" Proc. Int. Conf. Fundamental and applied MHD, Pamir 2011 V.1, p.257-260.- Borgo-Corsica-France September 5-9, 2011

Cooperation

1. ISTOK Lisbon, Portugal

3.2. Design and implementation of time resolved liquid metal vapor spectroscopy at tokamak FTU Frascati
WP-11-PWI-04-01 VR/BS

Principal investigator: I. Tale
Staff members: J. Butikova, A. Voitkans

Background

The liquid Ga metal limiter experiment will be provided in collaboration between three Associations: ENEA Frascatti, Italy, IST Lisbon, Portugal, AEUL, Latvia.

The goals for development of the Ga vapour spectroscopy at tokamak ENEA Frascati have been elaborated taking in account of the following results of experiments performed at tokamak IST, Portugal.

- The presence of the jet in the chamber generates a pronounced increase in the haracteristic emission of Ga vapor spectral lines. Evaporated Ga penetrates in the plasma and close to the jet surface is rapid ionized to higher ionization stages. (Ga, Ga^{+} and Ga^{2+} ionization potentials are respectively: 6.0, 20.5 and 30.7 eV).
- Penetration profiles of Ga and Ga ions in the plasma polodial plane are distinctive.
- Evaluation of the kinetics of Ga vapor concentration due to interaction with plasma shot serves important information for the Ga vapor creation and decay process.

According to the final plan the Ga multijet experiments at IST tokomak ISTTOK during 2010 are not performed.

Goals

1. Development of the methodology for evaluation of the vapor concentration from emission intensity data for impurity spectrosccopy at ENEA Frascati.
2. Testing of the methodology using results of spectroscopy of Ga- vapor emission lines at tokamak ISSTOK.

Results

Concept for estimation of Ga vapour concentration using Ga emission spectroscopy

Emission model of Ga vapors

- Metal impurities in Tokamak are excited and deexcited by collisions with the plasma electrons.
- Excitation and deexcitation rate is governed by the electron concentration an temperature.
- Electron excitation rate can be averaged over Maxwellian velocity distribution.

- Spontaneous emission between two Ga atom levels *m, n* will be observed in different ionization states.
- During the plasma pulse thermodynamic equilibrium exists between different Ga ionized states

Basic equations, Emission intensity

- Electron excitation rate averaged over Maxwellian velocity distribution

$$X_{mn} = 1.6x10^{-5}\,\frac{f_{mn} < g(n,m) > N_e}{\Delta E_{nm} T_e^{1/2}} \exp\left(-\frac{\Delta E_{nm}}{kT}\right)$$

where:

fnm- oscillator strength - spectroscopy tables of elements

<*g(n,m)*> -averaged Gaunt factor ~ 1 for atoms; ~ 0.2 for ions

Δ *Enm* = *En*-*Em* – *n*–th and *m*-th levels energy - spectroscopy tables of elements

Ne - electron concentration in plasma (in cm3) - plasma parameter

Te – electron temperature in plasma (in eV) - plasma parameter

- Electron deexcitation rate

$$Y_{nm} = \frac{N_m^*}{N_n^*} X_{mn}$$

where

$$N_m^* \Big/ N_n^* = \left(g_m \Big/ g_n\right) \exp \frac{\Delta E_{nm}}{kT_e}$$

- Rate for spontaneous decay *n* - *m* (Einstein *A* coefficient)

$$A_{nm} = 4.3x10^7 \, g_m \Big/ g_n \, f_{mn} \left(\frac{\Delta E_{nm}}{kT_e}\right), \quad \text{sec}^{-1}$$

- Intensity emitted per unit volume from the transition *n* to *m* on a optically thin plasma

$$I_{nm} = 1.6x10^{19} A_{nm} N_n \Delta E_{nm}, \ \text{Watt/cm}^3$$

- Condition for steady state in a corona model

$$n_0 N_e \left(\sigma_{0n} v\right) = N_n A_{n0}$$

- Intensity emitted per unit volume for transition *n – m*

$$I_{nm} = 5.1 \times 10^{-25} \, \frac{f_{nm} g_0 N_e N_0}{g_m T_e^{1/2}} \left(\frac{\Delta E_{nm}}{\Delta E_{n0}}\right)^3 \exp\left(-\frac{\Delta E_{n0}}{T_e}\right) \text{ watt/cm}^3,$$

Concentration of Ga atoms/ ions in plasma

$$\Rightarrow \quad \boxed{N_0 = 2\times 10^{24}\,\frac{I_{nm} g_m T_e^{1/2}}{f_{nm} g_0 N_e \left(\frac{\Delta E_{nm}}{\Delta E_{n0}}\right)^3 \exp\left(-\frac{\Delta E_{n0}}{T_e}\right)}} \quad \text{cm}^{-3}$$

Basic equations. Shell – shell ionization

Ionization from the ground state over Maxwellian electron distribution for $0.02 \le T_e / E_\infty^Z \le 100$.

Ionization rate S(Z):

$$S(Z) = 10^{-5}\,\frac{\left(T_e / E_\infty^Z\right)^{1/2}}{\left(E_\infty^Z\right)^{3/2}\left(6.0 + T_e / E_\infty^Z\right)} \exp\left(-\frac{E_\infty^Z}{T_e}\right) \text{ cm}^3/\text{sec},\ E_\infty^Z \text{ - ionization energy}$$

Steady state: $\frac{N_e N(Z)}{N(Z-1)} = \frac{S(Z-1)}{\alpha_3}$, $\Rightarrow$ $\boxed{N^*(Z) = \frac{N^*(Z-1)\times S(Z-1)}{\alpha_3 N_e}}$

$\alpha_3 = 8.75\times 10^{-27} T_e^{-4.5}$ = **2.8×10^{-31} cm^6/sec** (electron-ion recombinative rate)

Estimation of Ga vapour concentration using Ga emission spectroscopy

At present Ga vapor distribution in tokamak plasma have been performed only during single Ga jet experiments at ISTTOK. Distribution of GaI, GaII and GaIII emission in the polodial plane have bēen observed. The distribution shape depends on the Ga ionization step.

Using experimental data of the relative average intensity for GaI, GaII, GaIII distribution of Ga vapor concentration in different ionized states in the tokamak plasma in thermodynamic equilibrium.

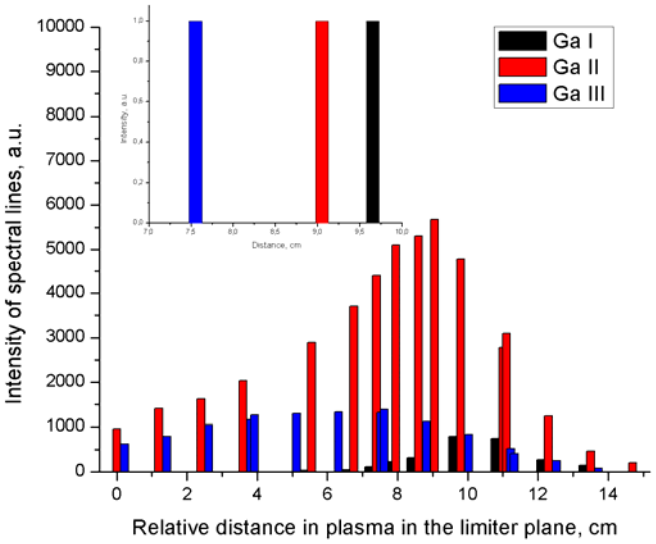

Fig.3.2.1.

We present the results for plasma parameters typical for TOKAMAK Frascatti, planned for investigation of liquid metal experiments.

Plasma parameters:

The Gaunthy factor representing the statistic weight of electron levels involved in transitions: $\langle g(n,0) \rangle \sim 0.2$

The electron temperature $T_e = 10$ eV

The plasma electron temperature $N_e = 0.55 \times 10^{20}$ m^3

Results

Concentration of Ga vapours in the first outer shell of Ga

Ga I	**Ga II**	**Ga III**
$I_{nm} = 20$ a.u.	$I_{nm} = 90$ a.u.	$I_{nm} = 5$ a.u.
$\mathbf{N_{GaI} = 5.1 \times 10^8\ m^3}$	$\mathbf{N_{GaII} = 7.6 \times 10^8\ m^3}$	$\mathbf{N_{GaIII} = 1.9 \times 10^8\ m^3}$

Concentration of Ga vapours in the inner shells (Saha equilibrium)

Ga IV

$N(Z-1) = N_{GaI} + N_{GaII} + N_{GaIII} = 1.4 \times 10^9\ m^3$

$\mathbf{N_{GaIV} = 2.6 \times 10^{10}\ m^3}$

Ga V

$\mathbf{N_{GaV} = 4.3 \times 10^9\ m^3}$

Ga VI

$\mathbf{N_{GaVI} = 2.7 \times 10^8\ m^3}$

Results are represented in table and Fig.3.2.2

	N_0, cm^{-3} Concentration	E_0, eV Ionisation energy	S(Z), cm^{-3}/sec Ionisation rate
Ga I	5.1×10^{8}	5.9	6.3×10^{-8}
Ga II	7.6×10^{8}	20.5	1.6×10^{-9}
Ga III	1.9×10^{8}	30.7	2.8×10^{-10}
Ga IV	2.6×10^{10}	63.2	2.4×10^{-12}
Ga V	4.3×10^{9}	86.0	1.3×10^{-13}
Ga VI	2.7×10^{8}	112.6	5.2×10^{-15}

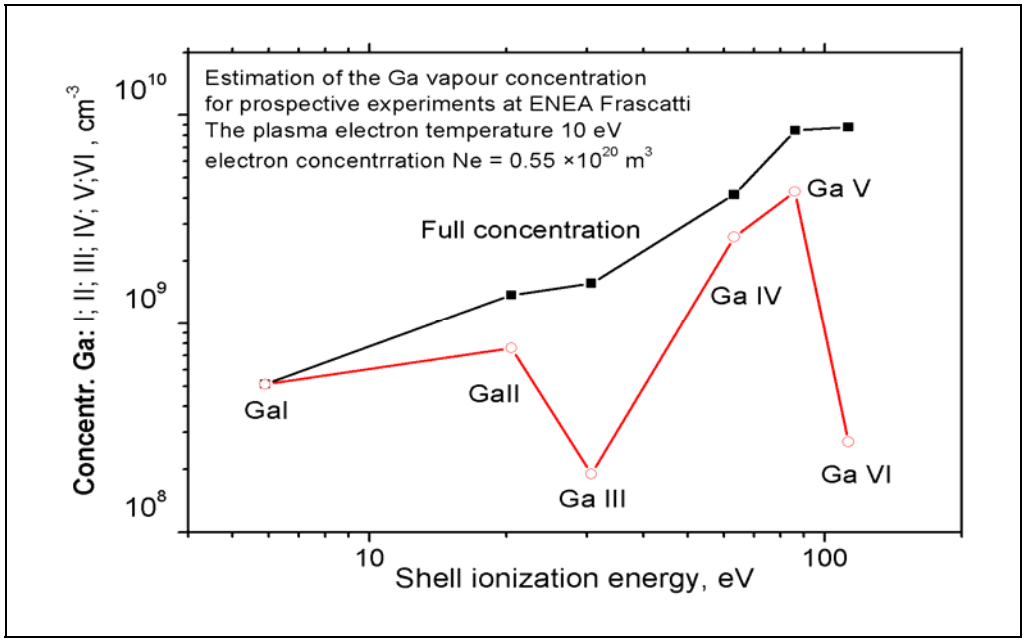

Fig . 3.2.2. Experimental concentration data for GaI, GaII,GaIII and calculated for GaIV, GaV and GaVI.

Using experimental data the actual full concentration of Ga wapours in the first shell is calculated. The maximum concentation show single ionized GaII.

Ga concentration data for the first shell are used to estimate full vapor concentration in plasma. Contribution by increase of *Z* vanes, the concentration saturates.

Conclusions

1. The developed routine for estimation of Ga vapour total concentration in plasma can be applied in the future experiments.
2. The routine can be applied for investigations of other liquid metal experiments (Li)

3. For Ga experiments the vapour concentration shall be performed up to the Ga IV (see table).
4. The routine can be applied for investigations of other liquid metal experiments (Li)
5. Independent plasma electron temperature distribution is required for investigation of Ga or other material distribution in radial and poloidal plaes, planed for installation at the tokamak Frascati.

Collaboration

1. FTU Frascati, Italia

3.3. Theory and code development

3.3.1. EU Topical Groups: TG-MHD (MHD), TG-H&CD (Heating and Current Drive)

Principal investigator O. Dumbrajs

Research Topics

3.3.1.1. Influence of possible reflections on the operation of European ITER gyrotrons

The theory describing the influence of reflections on operation of gyrotrons with radial output is used for evaluating the effect of reflections on the operation of the ITER 170 GHz 2 MW coaxial cavity gyrotron, which is under development, and the 170 GHz 1 MW cylindrical cavity gyrotron as a fall back solution.

3.3.1.2. Design of an optimized resonant cavity for a compact sub-Terahertz gyrotron

An optimized resonator is developed for a compact sub-Terahertz gyrotron to be used for plasma diagnostics. Instead of a regular (cylindrical) part as in the conventional cavities it contains an uptapered section. Such configuration offers a significant increase of the efficiency and improves the overall performance of the tube. We outline briefly the underlying theory, present and discuss the results of the numerical experiments carried out during the optimization process.

3.3.1.3. Numerical experiments with single mode gyrotron equations

Stationary and nonstationary problems in large time interval with complex oscillating initial conditions. Two versions of gyrotron equations are investigated.

3.3.1.4. A low-dimensional model system for quasi-periodic plasma perturbations

Large scale plasma instabilities not leading to an immediate termination of a discharge often result in periodic nonlinear perturbations of the plasma. A minimal possible model is formulated for description of the system with drive and relaxation processes which have different time scales. The model is based on two equations: the first being responsible for the relaxation dynamics and the second for the drive. The model can be generalized to describe the pellet injection.

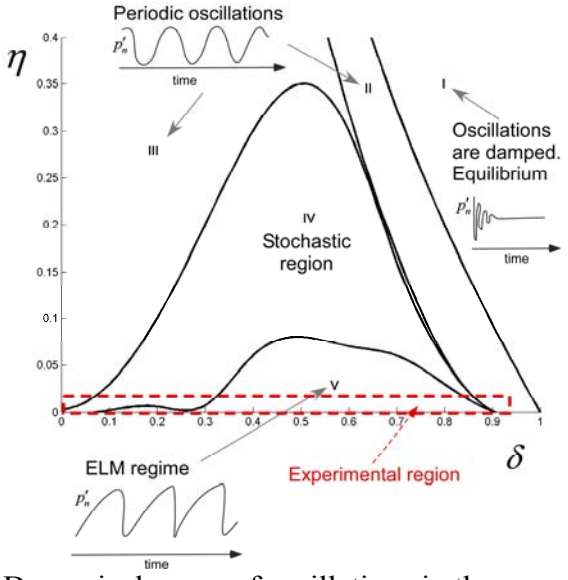

Fig. 3.3.1. Dynamical zones of oscillations in the parameter space.

3.1.1.5. Complex magnetohydrodynamic activities associated with a relaxation in HT-7 tokamak

A new relaxation instability with complex MHD activities is found in the HT-7 tokamak operational region, which manifests itself in bursts of hydrogen alpha-ray radiations, electron cyclotron emission and soft x-ray (SX) radiations on outer channels, as well as complex MHD perturbations, but without hard disruptions. The MHD modes are identified as m/n=2/1 m/n=3/2 and m/n=5/3 just before the relaxation (m and n are poloidal and toroidal mode numbers, respectively). The Poincare mapping, according to the measured perturbations of the MHD modes at the edge, is used to show the topology of magnetic field lines. It is found that a stochastic annular belt resulted just before the relaxation due to the m/n=5/3 island overlapping with m/n=2/1 and m/n=3/2 islands. This qualitatively coincides with the results of SX tomography.

Collaborators
EU Topical Groups: TG-MHD (MHD), TG-H&CD (Heating and Current Drive)
J. Cepitis, H. Kalis, A. Reinfelds (Institute of Mathematics and Computer Science of University of Latvia, **Latvia**).
Kaiyun Chen (Institute of Plasma Physics, Chinese Academy of Science, **China**).
D. Constantinescu (Faculty of Exact Sciences, University of Craiova, **Romania**).
Liqun Hu, Erzhong Li (Institute of Plasma Physics, Chinese Academy of Science, **China**).
T. Idehara (Far Infrared Center, University of Fukui, **Japan**).
V. Igochine, K. Lackner, R. Meyer-Spasche, H. Zohm (Max-Planck Institut für Plasmaphysik, Assotiation Euratom-IPP, **Germany**).
S. Sabchevski (Institute of Electronics of the Bulgarian Academy of Sciences, **Bulgaria**).

3.3.2. Computer modelling of impurity clusters in ODS steels

Principal investigator: Dr. V. Kuzovkov
Staff members: Yu.F. Zhukovskii, A. Gopejenko, Yu.A. Mastrikov,

Reduced activation ferritic-martensitic steels (RAFM) are promising structure materials for future fusion reactors. They possess better thermal conductivity, higher swelling resistance and lower damage accumulation than austenitic steels. Also these materials were developed to reduce the pollution and decrease the requirements for the facilities of the waste storage of the radioactive structures of the fusion reactors after service. Some elements that are contained in martensitic steels were substituted by other elements with faster decay of the induced radioactivity. One of the most used oxides used to reinforce RAFM steels is Y_2O_3. The RAFM steels strengthened by Y_2O_3 particles are being tested to evaluate the possibility of their implementation at temperatures of 650°C and higher instead of RAFM steels in combination with the advantages of the RAFM steels. Compared with the conventionally produced RAFM steels ODS RAFM steels have better tensile and creep properties.

The current study is aimed at simulation on atomic scale mechanisms of yttria particle nucleation and growth. For study of these mechanisms, it is necessary to investigate the interactions of yttrium solute atoms with vacancies and with oxygen atoms in interstitial positions as well as in substitute positions of Fe atoms. This stage requires systematic large-scale first principle calculations. The data set obtained at this stage is used for further kinetic Monte Carlo simulations of yttria particle nucleation and growth. Deep understanding of the kinetics of ODS particle formation gained in this project would support the new ways for further improvement of the properties of ODS steels advancing their development for fusion and numerous high-temperature applications as well as increasing their radiation resistance.

3.3.2.1. Simulations of inter-defect interactions in *fcc*-Fe lattice

The calculations on binding energies between either the Y and O substitute atoms or the two O substitute atoms have been performed. The largest binding energies have been obtained for pairs of atoms at 1-NN positions: 2.66eV and 2.03eV, respectively. With the increase of inter-defect distance, the corresponding binding energies decrease. When the substitutes are located at 4-NN positions, their bonding has been found either very low (for Y-O pair) or even negative (for O-O pair).

Binding energies between Y substitute atom and O located in octahedral interstitial site at various inter-atomic distances have been evaluated too. Yttrium atom has been placed in first, second and third coordination spheres around O atom. For the 1-NN configuration, the binding energy has been found to be negative, which is probably caused by the small distance between defect atoms as this configuration is energetically unfavourable. With the increase of the $Y\text{-}O_{int}$ distance the binding energy becomes positive and is approximately the same for the configurations where Y is located in the 2^{nd} and 3^{rd} coordiantation spheres around O atom and is equal to 0.38 and 0.42 eV respectively.

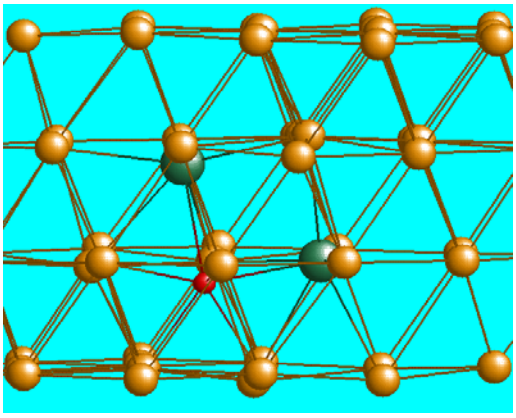

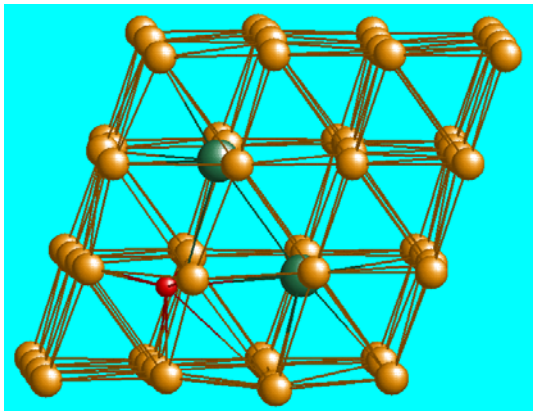

Figure 3.3.2.1. Relaxed (i) configuration of 2Y-O substitute atoms. **Figure 3.3.2.2. Relaxed (ii) configuration of 2Y-O substitute atoms.**

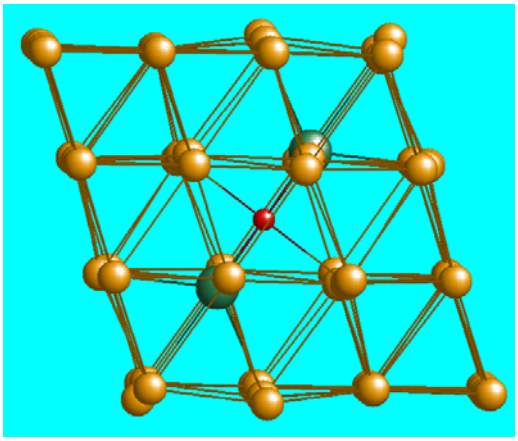

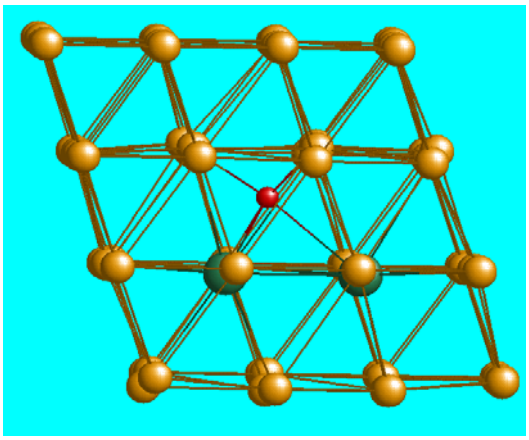

Figure 3.3.2.3. Relaxed (i) configuration of 2Y-O_{int} atoms. **Figure 3.3.2.4. Relaxed (ii) configuration of 2Y-O_{int} atoms.**

The calculations on different Y-O-Y cluster configurations (Figs. 1-4) clearly show that not only the presence of oxygen atom is required to form certain binding between impurity atoms but also the presence of Fe vacancies favors the growth of the Y_2O_3 precipitates inside the iron crystalline matrix. This has been proven by the calculations of interactions inside the Y-V_{Fe}-Y cluster for which the binding energy has been found to be rather large.

3.3.3.2. Simulations of inter-defect interactions in *bcc*-Fe lattice

We have performed also large-scale spin-polarized first principles calculations on impurities in the *bcc*-Fe matrix. ODS particles formation is mostly determined by mobility of Y atoms. Their diffusion in the Fe lattice occurs through vacancy mechanism. Initially, we have studied a pair of V_{Fe} at various distances one from another (Fig. 5a). At the next step, we began to construct a cluster of vacancies around Y atom, adding one vacancy at a time (Figs. 5b,c). We have found, that creation of such clusters is energetically favorable. We also have performed calculations on interstitial oxygen atom at octahedral and tetrahedral positions.

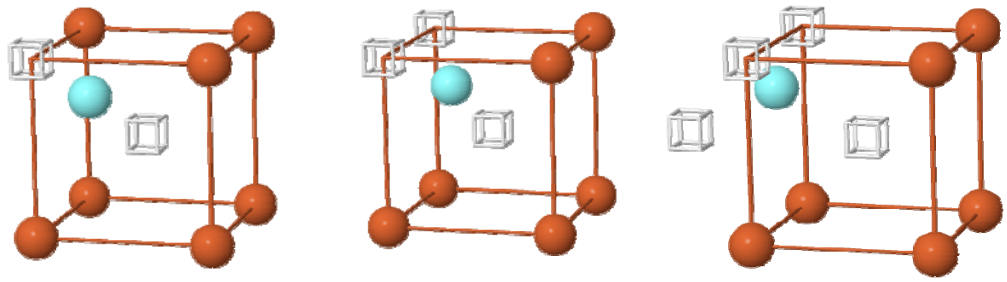

a) b) c)

Fig. 3.3.2.5. Three configurations of Y atom inside *bcc*-Fe lattice surrounded by two (a), three (b) and four (c) iron vacancies.

Collaboration

1. Karlsruhe Institute of Technology, Germany
2. Research Center Kurchatov Institute Moscow, Russia

4. EFDA FUSION TECHNOLOGY PROGRAMME

4.1. Distribution of tritium in the carbon based jet tiles

JW11-FT- 1.19

Principal investigator: G.Kizane
Staff members: M.Halitovs, A. Zarins, L. Baumane,J. Jansons, L.Avotina, B. Leshchinskis

Tritium accumulation in the fusion reactor is a problem that ought to be solved. First approach is an appropriate choice of materials and mitigation of its retention during operation.
Carbon fibre composite tiles were used for the first wall of the Join European Torus (JET). The erosion of the carbon of the first wall by D-T plasmas leads to a co-deposition of hydrogenated carbon films mainly on the colder parts of the surfaces of the plasma chamber because of a high affinity of carbon to hydrogen isotopes, neutron created structure damages causes tritium trapping effect and diffusion of tritium deeper in the bulk of material. The formation of such co-deposited tritiated layers and tritium retention in the bulk of constitutes ecological safety, decrease life time of materials. Tritium retention in the deposited layers and in the bulk of the CFC is very much influenced by various factors. Structure and chemical composition, energy of tritium ions, magnetic field and others are assumed to have an influence on tritium retention.

Investigations on the divertor samples of the largest fusion machine JET allow understanding fuel transport, understanding erosion process and formation of hydrocarbon films, tritium retention in the bulk of tiles and as result will give information for future fusion machines.

Analysis of selected samples of plasma-facing components CFC, in order to support particle transport studies, tritium trapping, development of in-situ detritiation methods and others has been proposed as the JET Fusion Technology activities in the frame of the EFDA 2011 Workprogramme.
In order to obtain wider information on tritium distribution, cooperation was realized between AEUL (Latvia) and MEdC (Romania) and TEKES (Finland) in the frame of the task JW11-FT-1.19. The full combustion measuring (FCM) in couple with liquid scintillation method has been realized in the AEUL and used for determination of tritium depth profiles, the investigations of properties of the tritium trapped in the surface layers and in the bulk of CFC's with respect to temperature, radiation and magnetic field. The samples were analysed by SIMS analysis in the laboratory of the TEKES and the Accelerator Mass Spectrometry (AMS) method was used in the AMS laboratory for T and D measurement in selected samples of tile. The AMS measurements reveal important information regarding the energy of the incoming particles bombarding the protection tiles in the Tokamak vessel. Information of localized tritium in an upper layer and depth of CFC is useful and will give additional

data for modeling fuel transport. Analysis in the frame of the tasks JW9-FT-3.46 and JW10-FT-3.62 were continued.

The aim of tasks is

- to organize tritium thermal desorption process in couple with simultaneous thermal analysis,
- to investigate release tritium under action of temperature, radiation and magnetic field separately and simultaneously,
- to analyze tritium distribution in the selected tile in both in poloidal and toroidal direction.

4.1.1. Experimental and results

The task JW11-FT-1.19, JW10-FT-3.62 and JW9-FT-3.46 are related to the estimation of the tritium distribution in the carbon based tiles and are continuation of the EFDA JET Technology Tasks on the tritium in tokamaks.

Goals of the task are to determine depth profiles of tritium trapped in the bulk of CFC tiles, make comparison of tritium activities in the bulk and surface layers, estimate changes of structure of a tile, to investigate properties of the tritium trapped in CFC tiles. Tile 14BWG4B and 14 ING3B (exposed in 2001-2004) from MK II SRP was analyzed for realization of the tasks because the tritium accumulation dominates on the inner divertor shadowed areas. The samples for analysis of tritium were prepared by standard methods and determination of tritium in a separate sample was realized by full combustion method and liquids scintillation method. In order to investigate the desorption of tritium under action of temperature, radiation and magnetic field separately or simultaneously annealing of the oblong CFC samples was performed in a continuous flow of the purge gas He + 0.1% H_2 of the rate 14-15 L/h with and without a magnetic field of 1.7 T and/or 5 MeV fast-electron radiation of the dose rate P=14 MGy·h^{-1} in a special radiation thermo-magnetic rig in Salaspils. Method of thermal analysis (TG/ DTA) of CFC samples connected with tritium monitor was adopted. Along with the experiments using the set-up that was put in our laboratory thermal desorption of tritium can be also performed by means of a state-of-the-art industrially-made thermal analyzer. Our laboratory tested a possibility to use a Seiko Instruments TG/DTA 6300 thermogravimetric/differential thermal analysis module for thermal desorption of tritium from a CFC sample.

Fig. 4.1.1 Positions of oblong samples 1-5, A1-A7, C1-C5 on the plasma-facing surface of tile 14BWG4B (a) and their initial total tritium surface activity in MBq·cm^{-2} (b). An oblong sample from row E was used for thermal desorption experiment with simultaneous thermal analysis.

4.1.2. Temperature programmed desorption with simultaneous thermal analysis

The temperature-programmed desorption spectrum of tritium from oblong sample E1 of tile 14BWG4B obtained by means of the thermal analyzer is shown in Fig. 4.1.2.

In Fig. 4.1.2. the temperature-programmed desorption spectrum of tritium from oblong sample E1 is combined with the results of its thermal analysis. The tritium release in the temperature range of 300-600 °C can be associated with the mass loss of about 0.2% from the initial mass of sample E1, but the tritium release in the temperature range of 600-900 °C was not accompanied by any appreciable mass loss. We may note that the set-up of the experiment had no zinc bed. Therefore, the possibly released tritiated water and some possibly released tritiated organic compounds may have been retained in the silica gel column and in the cold trap.

The residual tritium amount in sample E1 after the thermal desorption shown in Fig. 4.1.2 was determined by the full combustion method and was found to be 127 Bq, which is about 0.1% of the initial total amount, which is estimated to be about 125 kBq.

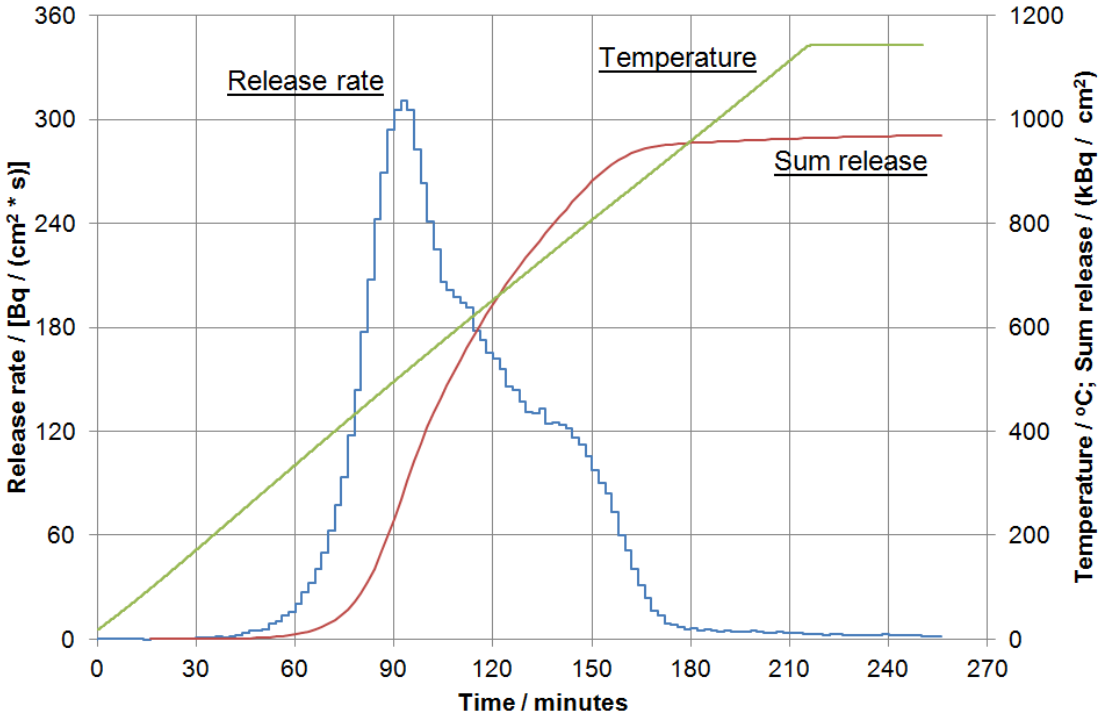

Fig. 4.1.2. Tritium release by thermal desorption from oblong sample E1 of tile 14BWG4B.

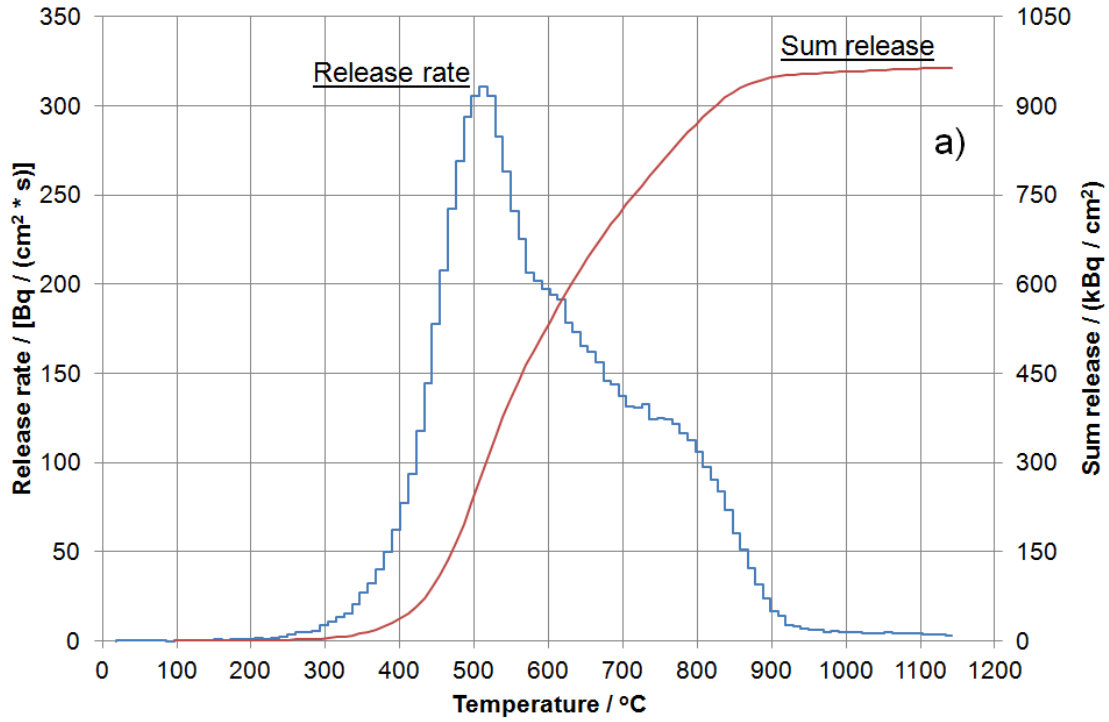
Release rate
Sum release
a)
Release rate / [Bq / (cm² * s)]
Sum release / (kBq / cm²)
Temperature / °C
0
50
100
150
200
250
300
350
0
150
300
450
600
750
900
1050
0
100
200
300
400
500
600
700
800
900
1000
1100
1200

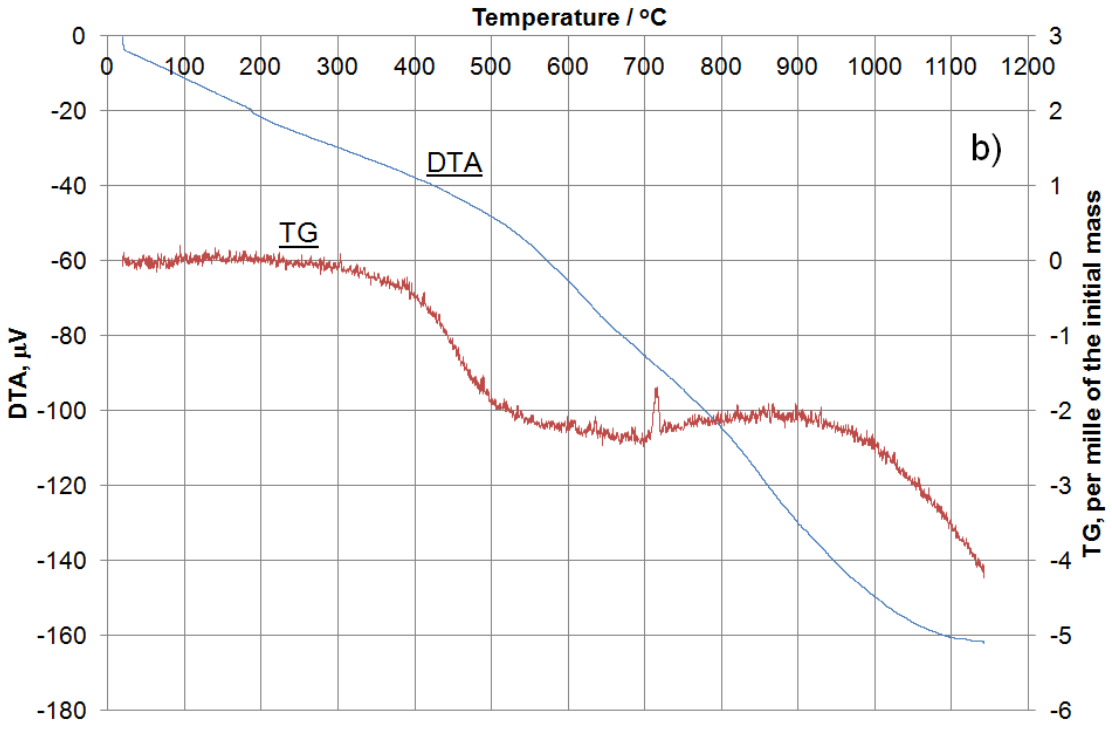
Temperature / °C
DTA
TG
b)
DTA, µV
TG, per mille of the initial mass
0
-20
-40
-60
-80
-100
-120
-140
-160
-180
3
2
1
0
-1
-2
-3
-4
-5
-6
0
100
200
300
400
500
600
700
800
900
1000
1100
1200

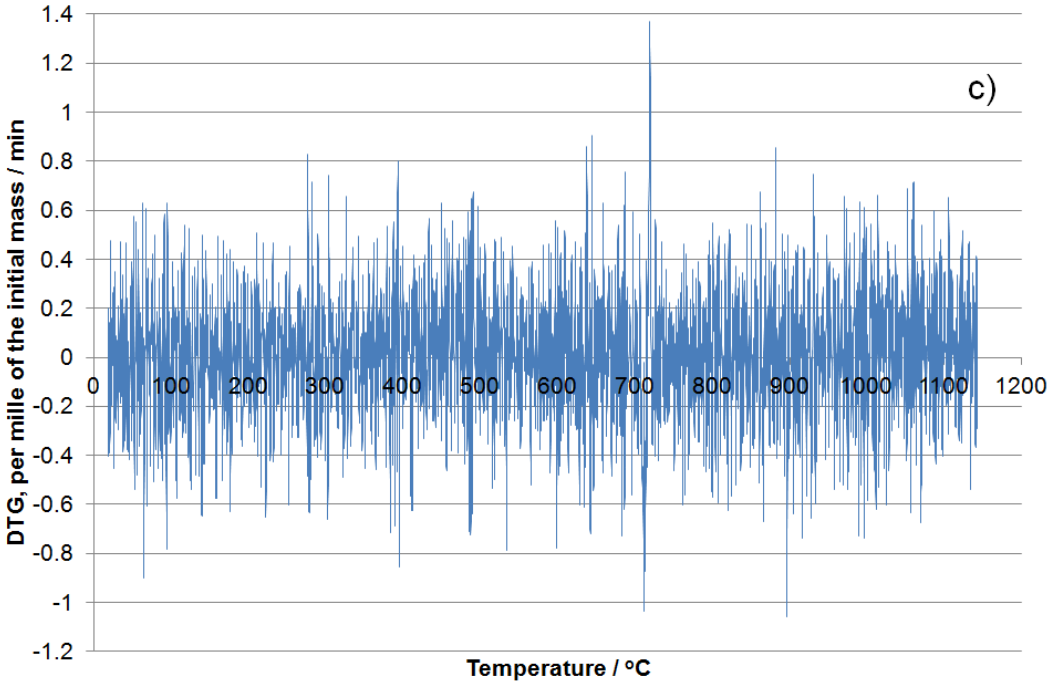

Fig. 4.1.3. Tritium release by thermal desorption from oblong sample E1 of tile 14BWG4B (a) and its simultaneous curves of differential thermal analysis (DTA), thermogravimetry (TG) (b) and differential thermogravimetry (TG).

4.1.3. The tritium release from untreated plasma exposed tiles under the simultaneous action of temperature, radiation and magnetic field

Investigations of properties of the tritium trapped in the deposited films, in the surface layers and in the bulk of PFCs with respect to temperature, radiation and magnetic field can contribute to the development of detritiation methods. In the year 2010 was determinate that most of tritium (89-99.9 %) is located in surface layer of the plasma-facing surface of tile 14BWG4B. Therefore from the viewpoint of the development of detritiation methods, we may expect that treatment of the plasma-facing surface of the tile with a detritiation technique will give a major contribution in the detritiation of the tile.

Tritium release at annealing for 180 min

Curves of the tritium release rate and sum release from oblong samples 5 and 4 of tile 14BWG4B (Fig. 4.1.1).under the action of electron radiation for 180 min with no additional heating are shown in Fig. 4.4. Most of that tritium was released during the first 30 min of electron irradiation. The last 120 min of the electron irradiation contributed little to the detritiation. Therefore, the further experiments were performed with the electron irradiation for 30 min. The final values of the tritium fractional release – 48% and 55% for samples 5 and 4 respectively – indicate the upper limit of the degree of detritiation achievable with the 5 MeV electron irradiation under the given conditions. After switching the electron radiation on, the temperature curves shown in Fig. 4.1.4. have a steep increase from room temperature to about 300 °C, and then they tend to reach a steady-state value with apparent variations, which are possibly related to the variations in the dose rate of the fast-electron beam. The maximum temperatures of 357 °C (sample 5) and 310 °C (sample

4) were reached after 110 min and 28 min respectively after switching the electron radiation on. Although sample 4 had similar or lower temperature than that of sample 5 during the electron irradiation, **the higher fractional release of tritium from sample 4 may testify a facilitating effect of a magnetic field of 1.7 T on the tritium release.**

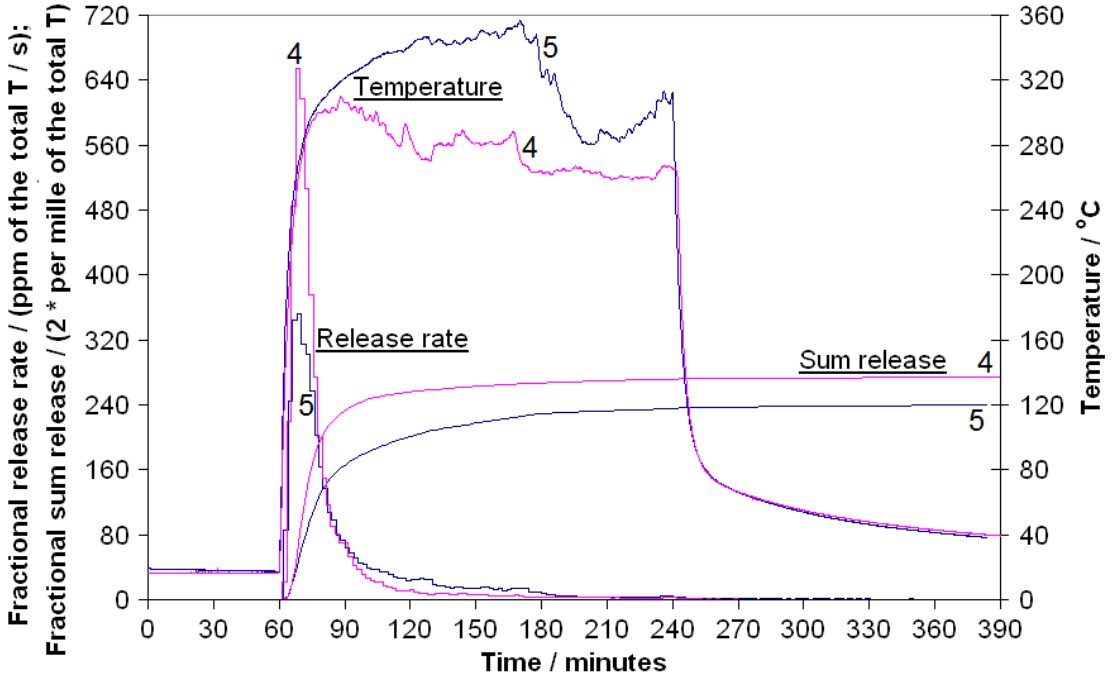

Fig. 4.1.4. Tritium release at annealing of oblong samples 5 and 4 in a continuous flow of 14-16 L/h of He + 0.1 % H_2 under the action of electron radiation for 180 min without additional heating, without magnetic field (sample 5) and with a magnetic field of 1.7 T (sample 4). The curves of the tritium fractional release have been calculated for the following values of the initial total tritium activity for 1 cm^2 of the plasma-facing surface, MBq·cm^{-2}: 5 – 0.472; 4 – 1.262.

By comparison, only 21% of the total tritium was released upon simple heating at 350-363 °C (sample 1, Fig. 4.1.5.). That is more than twice lower than that released under electron radiation (Fig. 4.1.5) at comparable or lower temperatures, indicating an additional facilitating effect of electron radiation on the tritium release in comparison with simple heating. In contrast to the tritium release under the electron radiation (Fig. 4.1.4), the curves of the tritium release rate have a sharp bend at the end of the temperature program (Fig. 4.1.5). That means that **a higher degree of detritiation might be achieved on heating for a longer time than that in Fig. 4.1.4.**

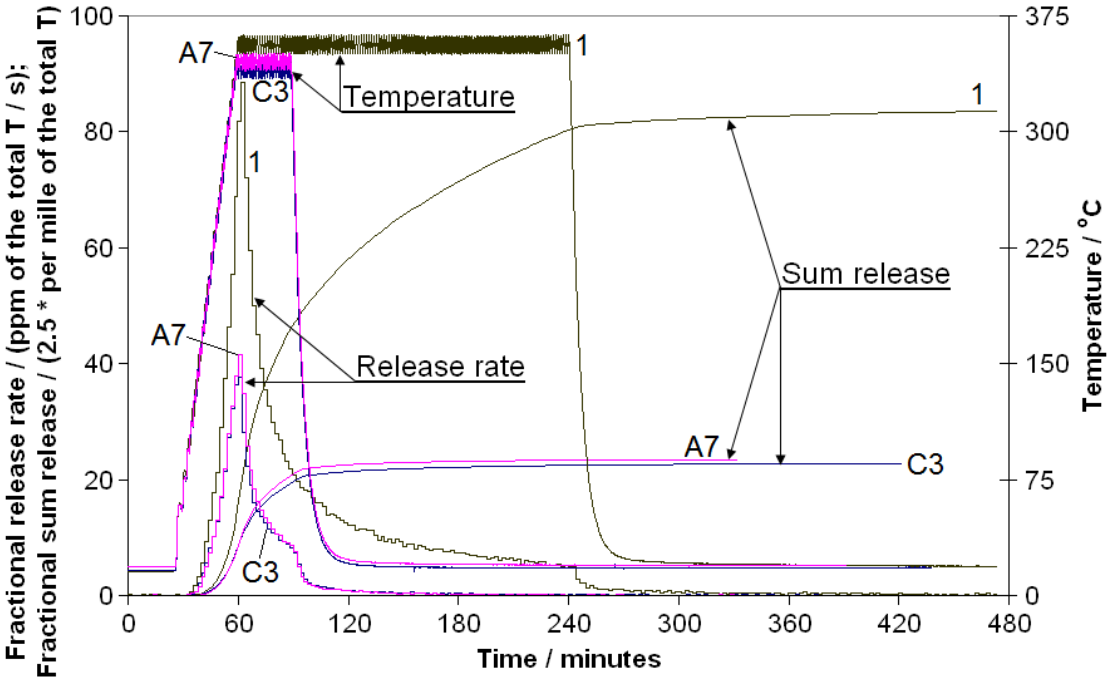

Fig. 4.1.5. Tritium release at annealing of oblong samples 1, C3 and A7 in a continuous flow of 14-16 L/h of He + 0.1 % H_2 at the given temperature programme without electron radiation and without magnetic field. The curves of the tritium fractional release have been calculated for the following values of the initial total tritium activity for 1 cm^2 of the plasma-facing surface, $MBq \cdot cm^{-2}$: 1 – 1.016; C3 – 2.952; A7 – 2.444.

Tritium release at annealing for 30 min

Curves of the tritium release rate and sum release from oblong samples 4 and 2 (Fig. 4.1.1) under the simultaneous action of electron radiation for 180 min and 30 min respectively and a magnetic field of 1.7 T with no additional heating are compared in Fig. 4.6. We can see that up to the 85th minute, when both the samples had reached 303 °C, the temperature of sample 4 was higher than that of sample 2, but sample 2 had to that time a higher fractional release of tritium (50%) than that of sample 4 (44%). Although sample 4 had been irradiated for a longer time (180 min) than sample 2 with a similar maximum temperature 310 °C at the irradiation, sample 2 had a higher final fractional release of tritium (61%) than sample 4 (55%). Both these facts testify that though samples 2 and 4 had similar values of the initial total tritium (1.07 and 1.26 MBq·cm^{-2} respectively), sample 4 had a more tightly bound tritium than sample 2. Therefore, we may conclude that the oblong samples studied had not only different values of the initial total tritium (0.47-3.53 MBq·cm^{-2} for all the 17 oblong samples studied, see below), but also they had different tritium release properties with respect to the released fraction under the given conditions.

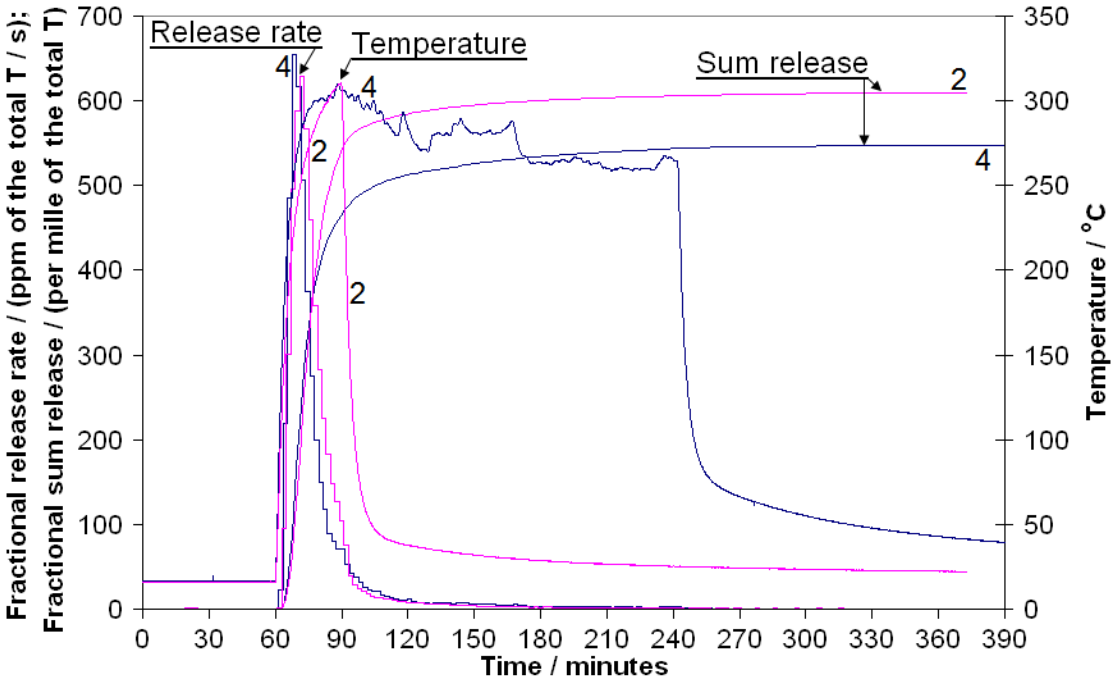

Fig. 4.1.6. Tritium release at annealing of oblong samples 4 and 2 in a continuous flow of 14-16 L/h of He + 0.1 % H_2 under the 5 MeV fast-electron irradiation for 180 min (sample 4) and 30 min (sample 2) without additional heating in a magnetic field of 1.7 T. The curves of the tritium fractional release have been calculated for the following values of the initial total tritium activity for 1 cm^2 of the plasma-facing surface, MBq·cm^{-2}: 4 – 1.262; 2 – 1.069.

Curves of the tritium release rate and sum release from oblong samples 5 and 3 (Fig. 4.1.1) under the action of electron radiation for 180 min and 30 min respectively without magnetic field and with no additional heating are compared in Fig. 4.7. We may note that samples 5 and 3 differed by a factor of > 7 with respect to their initial total tritium activity for 1 cm^2 of the plasma-facing surface – 0.47 and 3.53 MBq·cm^{-2} respectively. The **higher final value (48%)** of the tritium fractional sum release of sample 5 than that (32%) of sample 3 **is in agreement with the higher**

irradiation temperature and longer irradiation time for sample 5 that those of sample 3. In the case of sample 3, the second maximum of the tritium release rate is apparently caused by a sharp increase in the sample temperature possibly due to increase in the electron beam current. It is obvious from curve 3 of Fig. 4.1.7 that prolongation of the electron irradiation of sample 3 might considerably increase the tritium fractional sum release.

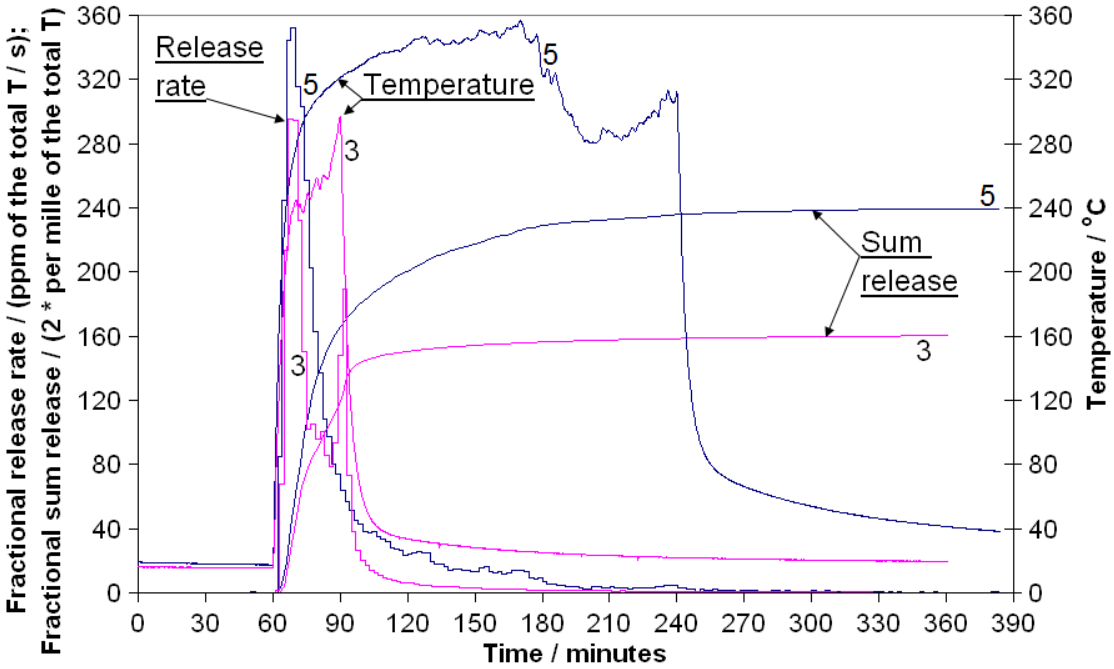

Fig. 4.1.7. Tritium release at annealing of oblong samples 5 and 3 in a continuous flow of 14-16 L/h of He + 0.1 % H_2 under the 5 MeV fast-electron irradiation for 180 min (sample 5) and 30 min (sample 3) without additional heating without magnetic field. The curves of the tritium fractional release have been calculated for the following values of the initial total tritium activity for 1 cm^2 of the plasma-facing surface, MBq·cm^{-2}: 5 – 0.472; 3 – 3.528.

Curves of the tritium release without and with magnetic field of 1.7 T are compared in Fig. 4.1.6**.** The comparison of the curves is limited by the fact that the sample temperature during most time of the irradiation without magnetic field (the maximum temperature 297 °C) was lower than that with magnetic field of 1.7 T (the maximum temperature 310 °C). Only in the beginning up to the time 70.43 min (the irradiation time 10.43 min) sample 3 has a higher temperature than sample 2. Up to the time 69 and 71 min, sample 3 released 6.9% and 10.5%, and sample 2 released 10.7% and 17.8% of the total tritium respectively as the tritium activity was recorded repeatedly after the measuring time of 2 minutes. The higher values of the tritium fractional release of sample 2 than those of sample 3 may **indicate that the magnetic field can enhance the tritium release.**

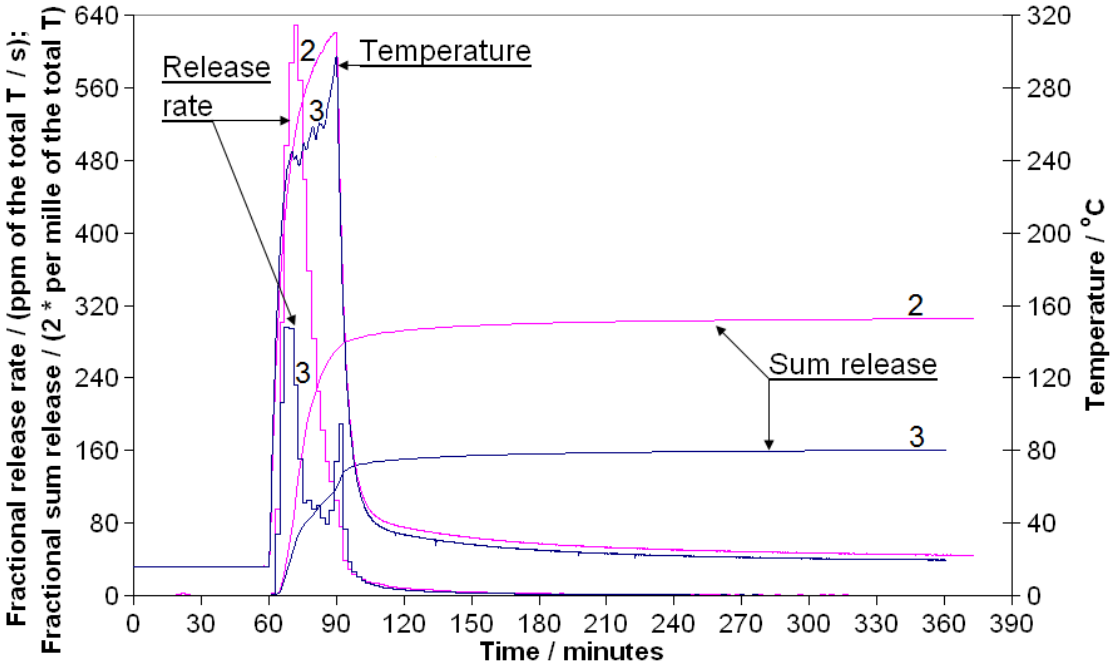

Fig. 4.1.8. Tritium release at annealing of oblong samples 2 and 3 in a continuous flow of 14-16 L/h of He + 0.1 % H_2 under the 5 MeV fast-electron irradiation for 30 min without additional heating in a magnetic field of 1.7 T (sample 2) and without magnetic field (sample 3). The curves of the tritium fractional release have been calculated for the following values of the initial total tritium activity for 1 cm^2 of the plasma-facing surface, $MBq \cdot cm^{-2}$: 2 – 1.069; 3 – 3.528.

Tritium fractional release curves from oblong samples 3 and C1 under the electron irradiation for 30 min are compared in Figs. 4.1.9. and 4.1.10. The maximum temperature of samples 3 and C1 at the electron irradiation was very similar – 297 and 298 °C respectively, but sample 3 had more than twice higher final fractional release (32.0%) than sample C1 (11.7%). In Fig. 4.1.9, the release curves are compared for the start of the electron radiation at the 60^{th} minute for both the samples. In Fig. 4.1.10, the start of the electron radiation is at the 60^{th} and 49^{th} minute for samples 3 and C1 respectively so that up to the time 79.55 min the temperature of sample C1 is higher than that of sample 3. Although the temperature of sample C1 was higher than that of sample 3, sample C1 released to the time 79 min (Fig. 4.1.9) less than 8.45% of the initial total tritium, but sample 3 released 17.55% to that time. That testifies that samples 3 and C1 were different not only by their initial total tritium (3.53 and 2.51 $MBq \cdot cm^{-2}$ respectively), but also by their fractional tritium release under the given conditions.

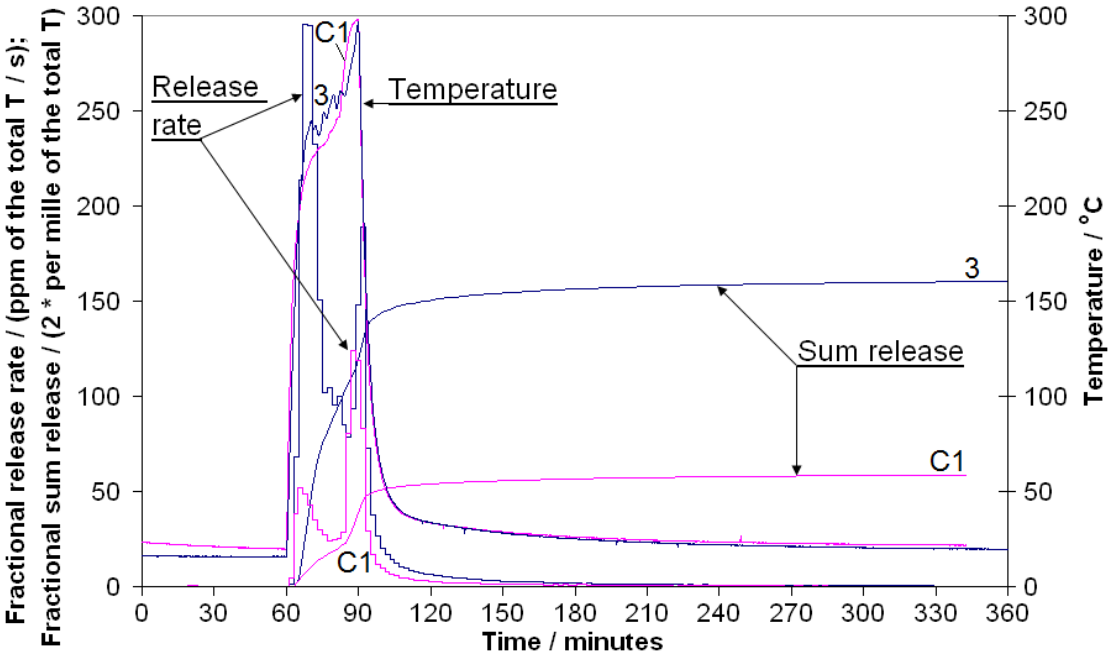

Fig. 4.1.9. Tritium release at annealing of oblong samples 3 and C1 in a continuous flow of 14-15 L/h of He + 0.1 % H_2 under the electron irradiation for 30 min without additional heating and without magnetic field. The release curves are compared for the start of the electron radiation at the 60th minute for both the samples. The curves of the tritium fractional release have been calculated for the following values of the initial total tritium activity for 1 cm^2 of the plasma-facing surface, MBq·cm^{-2}: 3 – 3.528; C1 – 2.505.

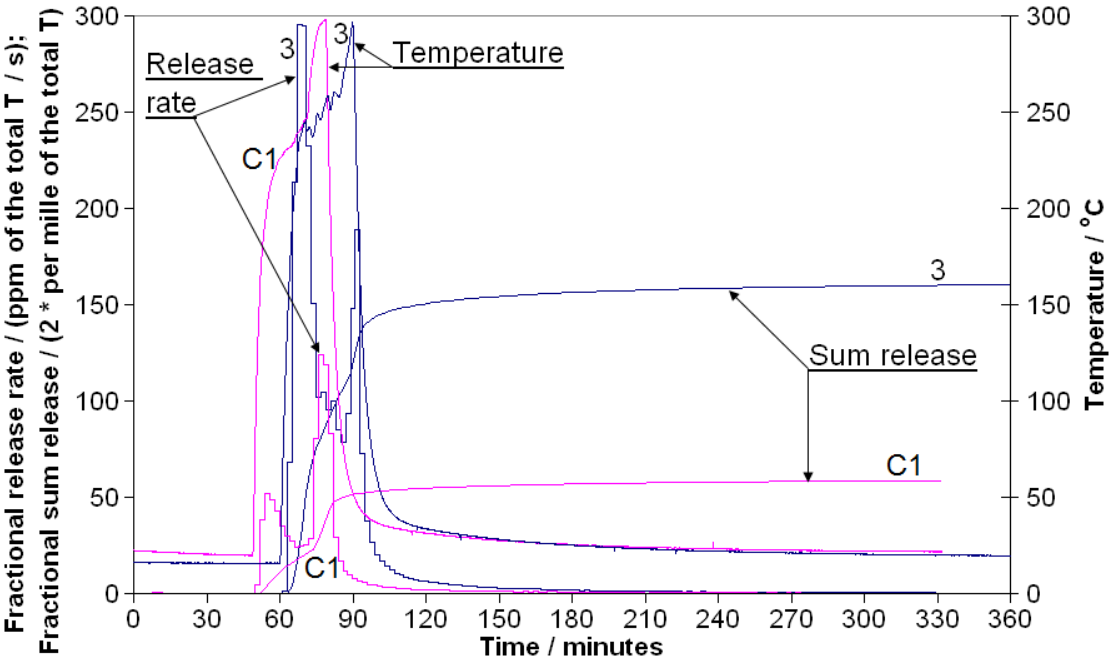

Fig. 4.1.10. Tritium release at annealing of oblong samples 3 and C1 in a continuous flow of 14-15 L/h of He + 0.1 % H_2 under the electron irradiation for 30 min without additional heating and without magnetic field. The start of the electron radiation is at the 60th and 49th minute for samples 3 and C1 respectively. The curves of the tritium fractional release have been calculated for the following values of the initial total tritium activity for 1 cm^2 of the plasma-facing surface, MBq·cm^{-2}: 3 – 3.528; C1 – 2.505.

Tritium fractional release curves from oblong samples A3 and C1 under the electron irradiation for 30 min are compared in Fig.4.1.11. The current collected with the probe adjacent to the electron-beam channel of ∅20 mm in the electromagnet pole was recorded manually. The sharp increase in the temperature of sample C1 at the end of the electron irradiation is apparently related to the increase in the electron beam current indicated by means of the current collected with the probe. It is worth noting that within the last 6 minutes of the electron irradiation though the probe current for sample C1 was similar or lower than that for sample A3, sample C1 has a higher temperature than sample A3 – their maximum temperatures were 298 and 276 °C respectively. A possible reason of the higher temperature of sample C1 than that of sample A3 at the end of irradiation may be the fact that sample C1 was larger in size and had a larger mass than sample A3 – their masses were 0.113 and 0.079 g respectively, and therefore sample C1 may have a larger absorption of the fast electrons in the case of a similar beam current.

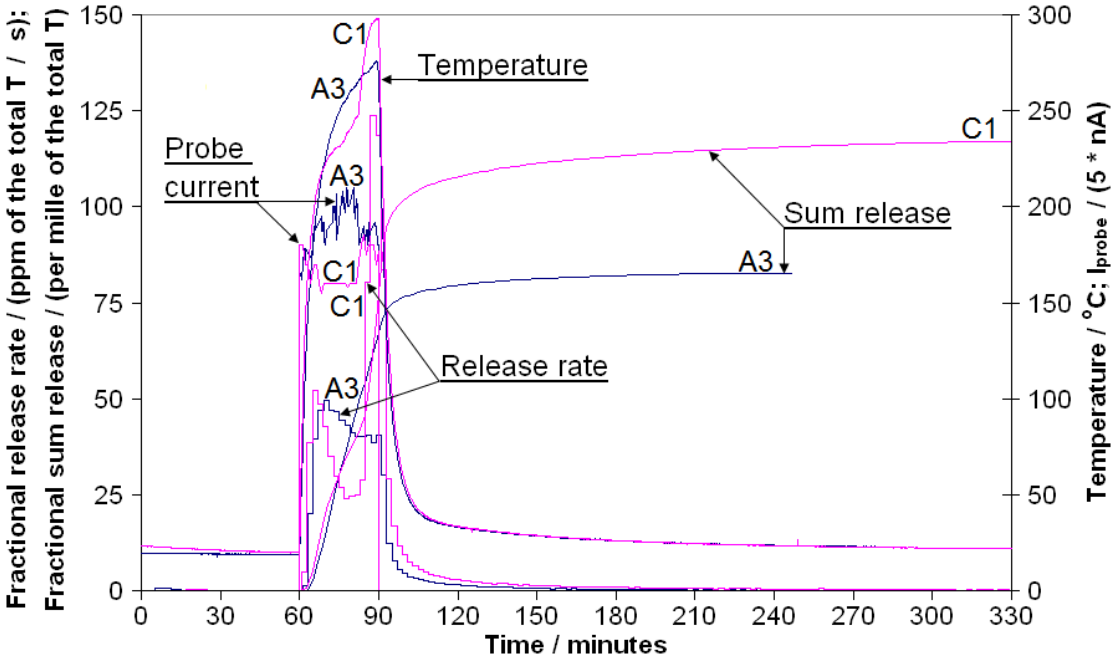

Fig. 4.1.11. Tritium release at annealing of oblong samples A3 and C1 in a continuous flow of 14-15 L/h of He + 0.1 % H_2 under the electron irradiation for 30 min without additional heating and without magnetic field. The curves of the tritium fractional release have been calculated for the following values of the initial total tritium activity for 1 cm^2 of the plasma-facing surface, MBq·cm^{-2}: A3 – 2.643; C1 – 2.505. The total charge of the current collected with the probe during the irradiation, mC: A3 – 1.70; C1 – 1.50.

Comparison of the tritium release from samples C4 and A1 in Fig. 4.1.12. shows a higher fractional tritium release from sample C4 than that from sample A1 though the temperature of sample C4 was similar or lower than that of sample A1, and, according to the current collected with the probe, the beam current for sample C4 also was lower than that for sample A1. That testifies that samples C4 and A1 are not only different by their total tritium content, 1.74 and 2.77 MBq·cm^{-2}, but also by their tritium release properties regarding their fractional release of tritium. Considering the relationship between the probe current and the sample temperature in Fig. 4.1.12, we may note that sample C4 had a slightly larger mass, larger plasma-facing surface and lesser thickness (0.095 g, 26.1 mm^2, 2.26 mm) than sample A1 (0.088 g, 20.6 mm^2,

2.72 mm). Variations in the sample size may be a reason of different sample temperature for the given electron beam current.

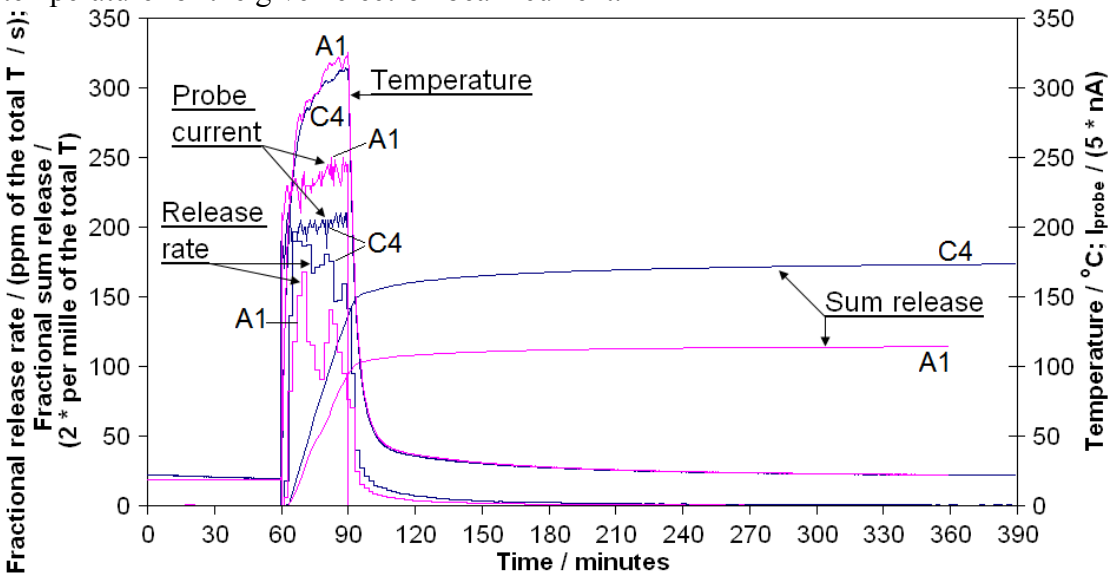

Fig. 4.1.12. Tritium release at annealing of oblong samples C4 and A1 in a continuous flow of 14-15 L/h of He + 0.1 % H_2 under the electron irradiation for 30 min without additional heating and without magnetic field. The curves of the tritium fractional release have been calculated for the following values of the initial total tritium activity for 1 cm^2 of the plasma-facing surface, MBq·cm^{-2}: C4 – 1.736; A1 – 2.768. The total charge of the current collected with the probe during the irradiation, mC: C4 – 1.80; A1 – 2.09.

Sample C4 released also a larger fraction (34.7%) of the total tritium than sample A6 did (22.7%) though the values of the initial total tritium activity (1.74 and 1.68 MBq·cm^{-2}), the probe current (the total charge at the irradiation: 1.80 and 1.83 mC) and the sample temperature (the maximum temperature: 314 and 310 °C) were similar (Fig. 4.1.13). Thus with respect to the fractional release, sample C4 had a larger fraction of loosely-bound tritium than samples A1 and A6. Though sample A1 had a higher maximum temperature (325 versus 310 °C) and a higher probe current (2.09 vs. 1.83 mC) than sample A6, samples A1 and A6 had very similar final fractions of the released tritium – 22.8% and 22.7% respectively (Fig. 4.1.14). Thus **with respect to the fractional release under the given conditions, samples A1, A6 and C4 can be arranged in the following sequence A1 ≤ A6 < C4,** where sample A1 had a similar or lesser fraction of loosely-bound tritium than sample A6, and sample C4 had a considerably larger fraction of loosely-bound tritium than samples A1 and A6.

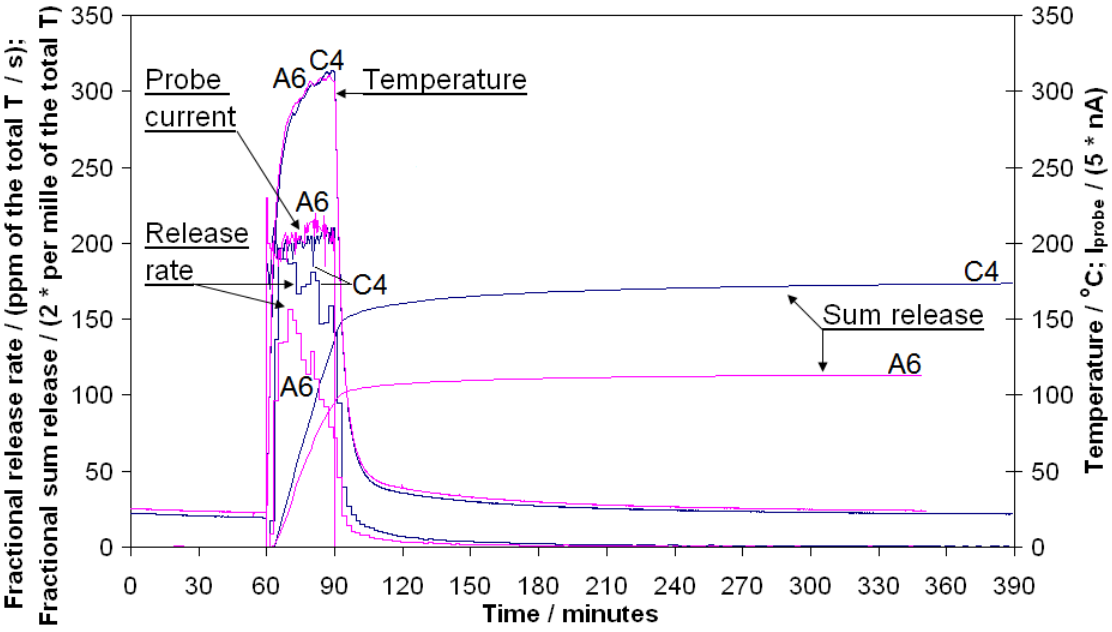

Fig. 4.1.13. Tritium release at annealing of oblong samples C4 and A6 in a continuous flow of 14-15 L/h of He + 0.1 % H_2 under the electron irradiation for 30 min without additional heating and without magnetic field. The curves of the tritium fractional release have been calculated for the following values of the initial total tritium activity for 1 cm^2 of the plasma-facing surface, MBq·cm^{-2}: C4 – 1.736; A6 – 1.676. The total charge of the current collected with the probe during the irradiation, mC: C4 – 1.80; A6 – 1.83.

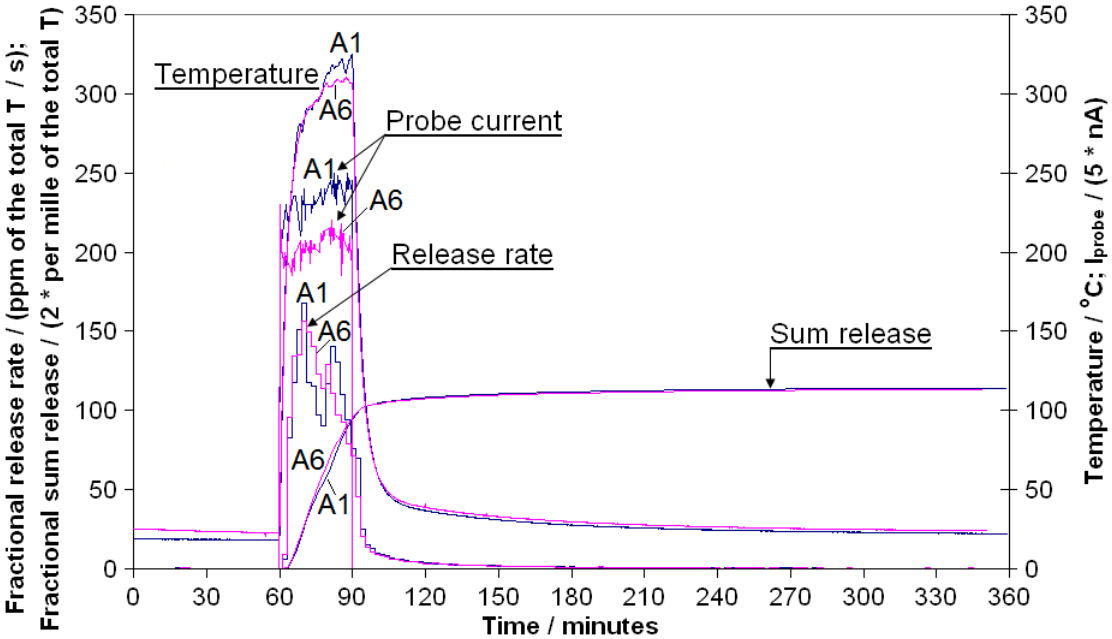

Fig. 4.1.14. Tritium release at annealing of oblong samples A1 and A6 in a continuous flow of 14-15 L/h of He + 0.1 % H_2 under the electron irradiation for 30 min without additional heating and without magnetic field. The curves of the tritium fractional release have been calculated for the following values of the initial total tritium activity for 1 cm^2 of the plasma-facing surface, MBq·cm^{-2}: A1 – 2.768; A6 – 1.676;. The total charge of the current collected with the probe during the irradiation, mC: A1 – 2.09; A6 – 1.83.

Regarding the possible effect of magnetic field on the tritium release, the pairs of adjacent oblong samples C4&C5, A1&A2 and A5&6 are compared in Figs. 4.1.15-4.1.17 Adjacent samples may be thought to be similar in respect of their tritium release properties. Sample C5 had a slightly lower probe charge (1.78 vs. 1.80 mC), a lower maximum temperature (292 vs. 314 °C) and a slightly lower final value of the tritium fractional release – 32.0% vs. 34.7% than sample C4 (Fig. 4.1.15). Though samples C4 and C5 are adjacent samples, their initial total tritium surface activity are different by a factor of about 2 – 1.74 and 3.44 MBq·cm^{-2} respectively. Comparison of samples A1 and A2 gives similar results. Sample A2 had a slightly larger probe charge (2.11 vs. 2.09 mC), a lower maximum temperature (284 vs. 325 °C) and a slightly lower final value of the tritium fractional release – 21.9% vs. 22.8% than sample A1 (Fig. 4.1.16). The adjacent samples A1 and A2 are different by their initial total tritium surface activity – 2.77 and 1.90 MBq·cm^{-2} respectively. Though the samples in the pairs C4&C5 and A1&A2 had similar size, the reason why the sample temperature was lower in a magnetic field of 1.7 T than that without magnetic field at similar values of the probe current (Figs. 4.1.15 and 4.1.16) is not clear. A possible reason of the lower temperature in the case of a magnetic field of 1.7 T may be focusing of the electron beam from the edge to the centre by magnetic field, and, therefore, a larger actual temperature gradient between the sample and the thermocouple may be present in a magnetic field of 1.7 T in comparison to the experiment without magnetic field.

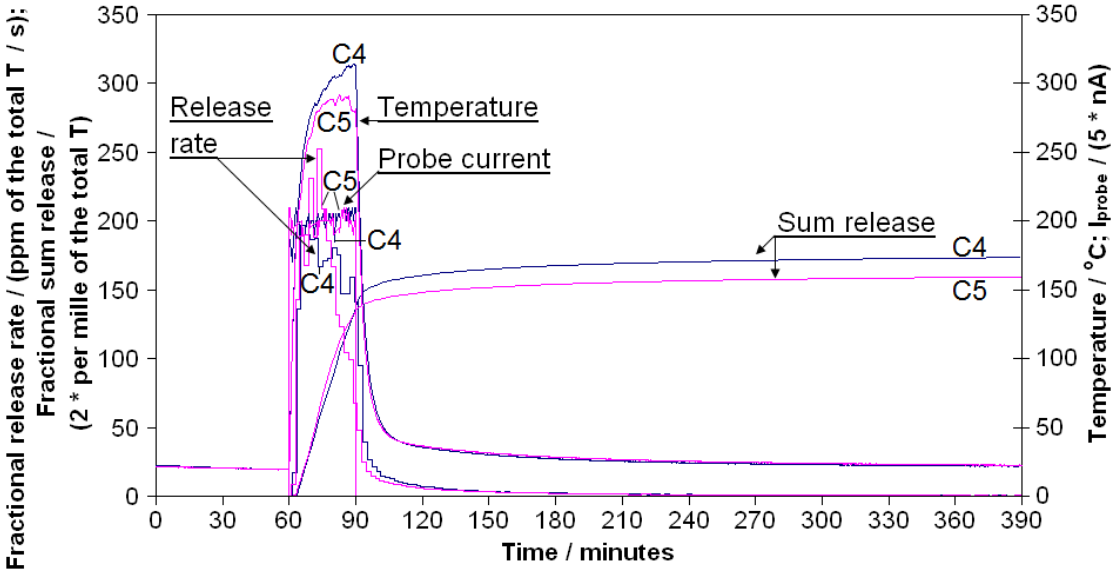

Fig. 4.1.15. Tritium release at annealing of oblong samples C4 and C5 in a continuous flow of 14-15 L/h of He + 0.1 % H_2 under the 5 MeV fast-electron irradiation for 30 min without additional heating in a magnetic field of 1.7 T (sample C5) and without magnetic field (sample C4). The curves of the tritium fractional release have been calculated for the following values of the initial total tritium activity for 1 cm^2 of the plasma-facing surface, MBq·cm^{-2}: C4 – 1.736; C5 – 3.436. The total charge of the current collected with the probe during the irradiation, mC: C4 – 1.80; C5 – 1.78.

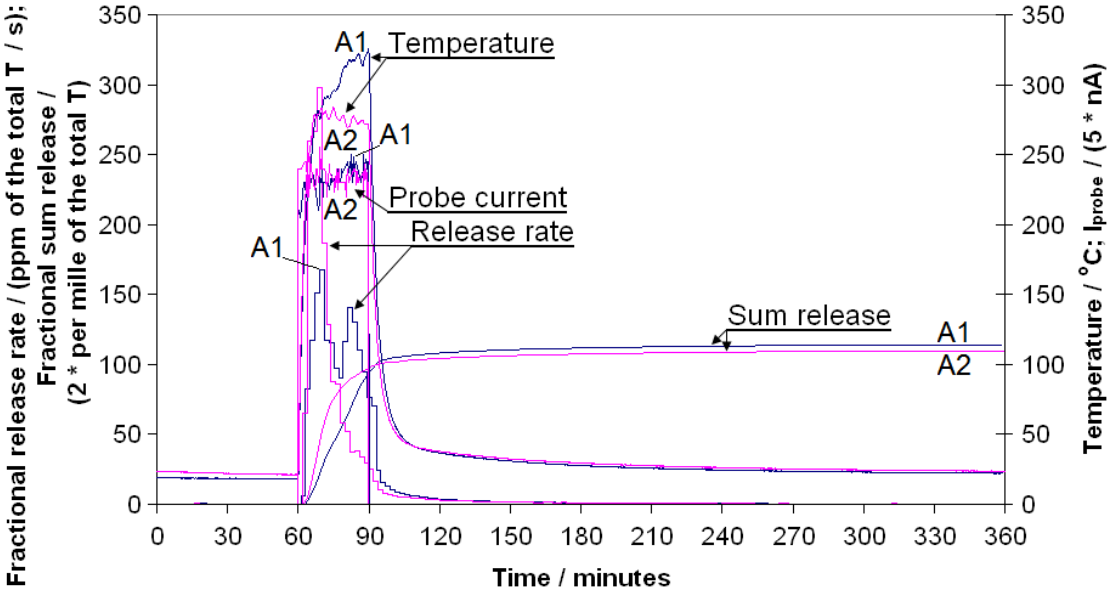

Fig. 4.1.16. Tritium release at annealing of oblong samples A1 and A2 in a continuous flow of 14-15 L/h of He + 0.1 % H_2 under the 5 MeV fast-electron irradiation for 30 min without additional heating in a magnetic field of 1.7 T (sample A2) and without magnetic field (sample A1). The curves of the tritium fractional release have been calculated for the following values of the initial total tritium activity for 1 cm^2 of the plasma-facing surface, $MBq \cdot cm^{-2}$: A1 – 2.768; A2 – 1.904. The total charge of the current collected with the probe during the irradiation, mC: A1 –2.09; A2 – 2.11.

Comparison of the adjacent samples A5 and A6 gives evidence of a facilitating magnetic field effect on the tritium fractional release (Fig. 4.1.17). Though sample A5 had a slightly lower probe charge (1.75 vs. 1.83 mC) and a lower maximum temperature (303 vs. 310 °C) than sample A6, sample A5 in a magnetic field of 1.7 T had a larger final released fraction of the total tritium (28.2% vs. 22.7%) than sample A6 without magnetic field (Fig. 4.1.17).

The tritium release experiment with sample A4 was initially planned as an experiment in a magnetic field of 1.7 T. However, a section of the electromagnet coil was unintentionally externally short-circuited by a loose aluminium outer cover of the coil during the electron irradiation of sample A4. Therefore, though the electromagnet current increased from 61 A to 140 A because of the short-circuit, and then in the 68th minute was deliberately diminished to the lowest value of 96-94 A allowed by the direct-current power supply with step-wise regulation, we may expect that the actual value in the interpolar space was lower than 1.7 T because of a diminished number of turns of the electromagnet coil. Comparison of the adjacent samples A4 and A5 in Fig. 4.1.16 shows a larger final tritium fractional release of sample A5 in a magnetic field of 1.7 T (28.2% vs. 17.8%) though the probe charge and the maximum temperature were similar in both the experiments – 1.71 and 1.75 mC, and 301 and 303 °C for samples A4 and A5 respectively.

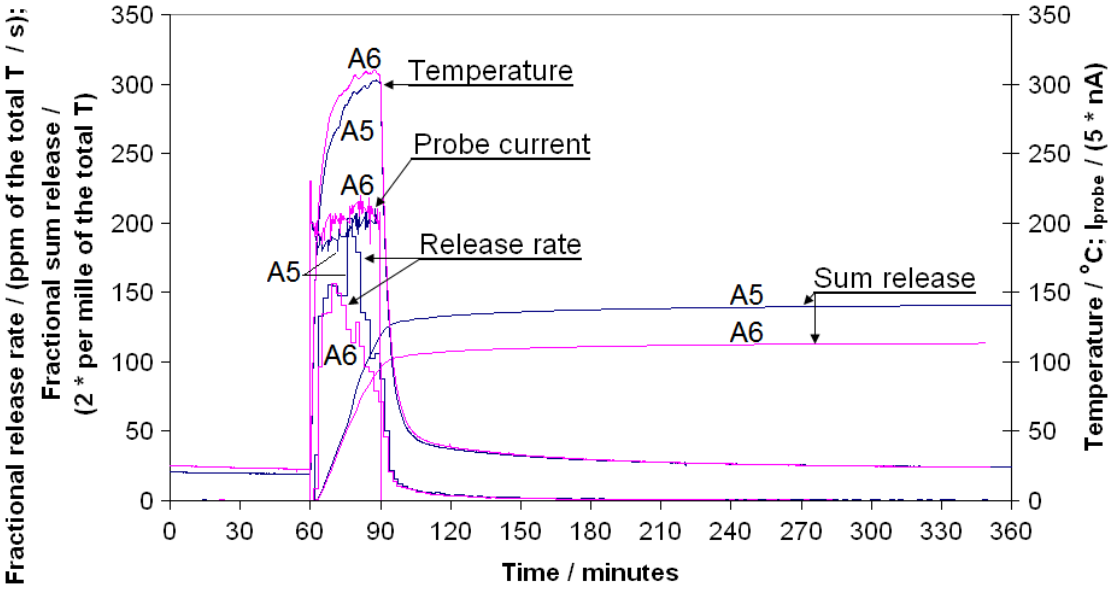

Fig. 4.1.17. Tritium release at annealing of oblong samples A5 and A6 in a continuous flow of 14-15 L/h of He + 0.1 % H_2 under the 5 MeV fast-electron irradiation for 30 min without additional heating in a magnetic field of 1.7 T (sample A5), without magnetic field (sample A6). The curves of the tritium fractional release have been calculated for the following values of the initial total tritium activity for 1 cm^2 of the plasma-facing surface, MBq·cm^{-2}: A5 – 1.535; A6 – 1.676. The total charge of the current collected with the probe during the irradiation, mC: A5 – 1.75; A6 – 1.83.

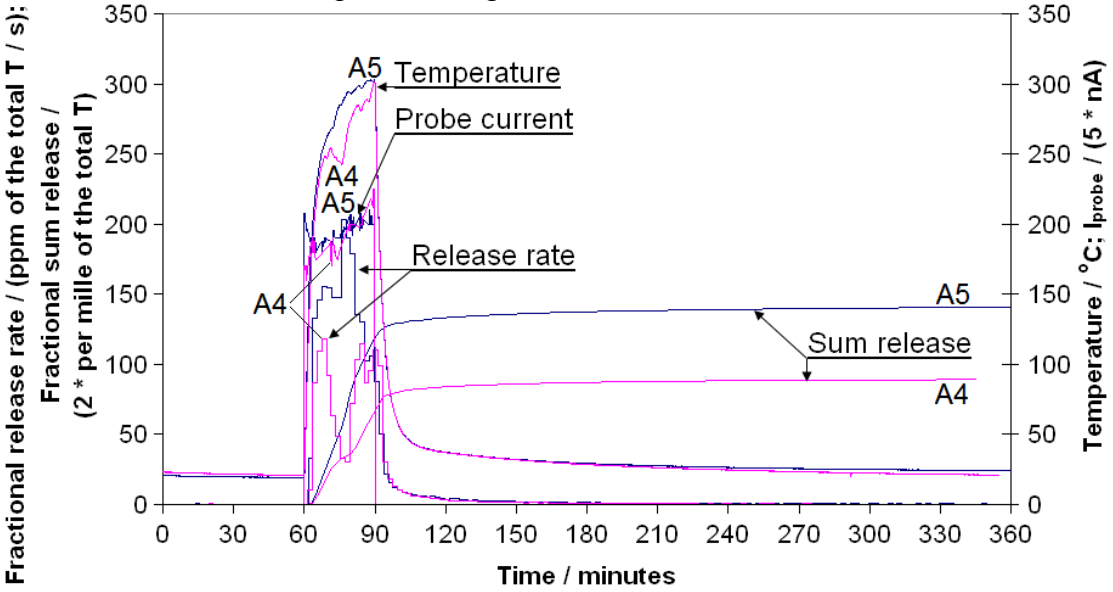

Fig. 4.1.18. Tritium release at annealing of oblong samples A5 and A4 in a continuous flow of 14-15 L/h of He + 0.1 % H_2 under the 5 MeV fast-electron irradiation for 30 min without additional heating in a magnetic field of 1.7 T (sample A5) and in a magnetic field of unknown intensity (sample A4). The curves of the tritium fractional release have been calculated for the following values of the initial total tritium activity for 1 cm^2 of the plasma-facing surface, MBq·cm^{-2}: A5 – 1.535; A4 – 1.618. The total charge of the current collected with the probe during the irradiation, mC: A5 – 1.75; A4 – 1.71.

From the viewpoint of similar patterns of the probe current and the sample temperature, it is also relevant to compare samples A1 and C2 (Fig. 4.19). Though

samples A1 and C2 had similar values of the probe charge (2.09 and 1.99 mC respectively) and the maximum temperature (325 and 324 °C respectively), sample **C2 in a magnetic field of 1.7 T had by a factor of about 3 larger final value of the tritium fractional release than sample A1 without magnetic field – 66.0% and 22.8% respectively**. This comparison may serve as an evidence of the facilitating magnetic field effect on the tritium release.

Investigation of the tritium release from samples C3 and A7 upon heating for 30 min without electron irradiation and without magnetic field (Fig. 4.5.) shows lower final values of the tritium fractional release (5.7% and 5.9% respectively) than those in the experiments with the electron irradiation (8.3-34.7%) though the temperature of samples C3 and A7 (334-346 °C and 340-351 °C respectively during the annealing for 30 min) was higher than those of the samples during the electron irradiation. Therefore, the electron irradiation had higher detritiation efficiency for the similar sample temperature than simple thermal treatment of the same duration without electron irradiation.

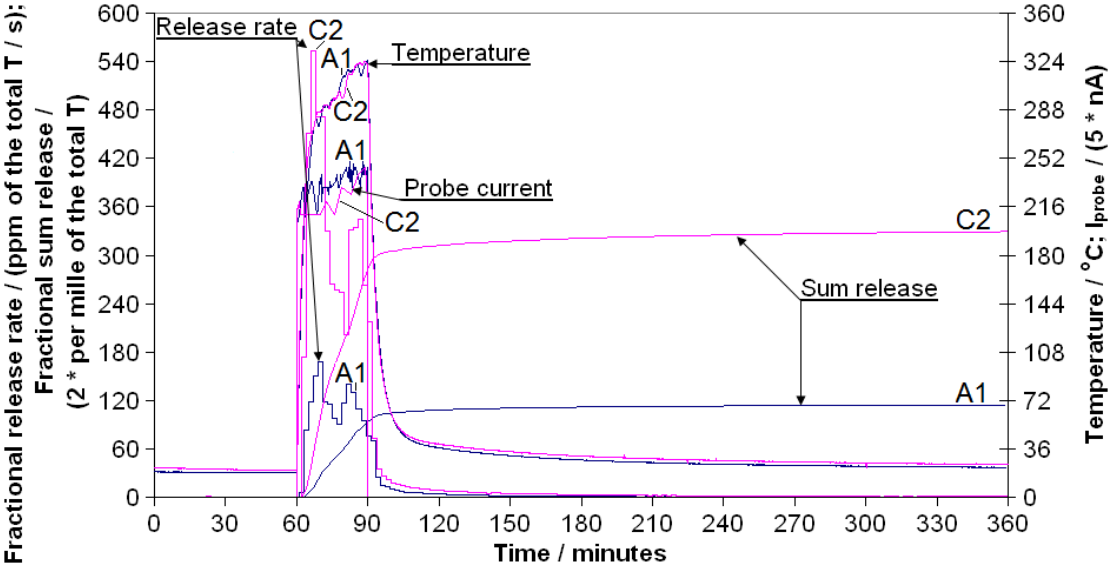

Fig. 4.1.19. Tritium release at annealing of oblong samples A1 and C2 in a continuous flow of 14-15 L/h of He + 0.1 % H_2 under the 5 MeV fast-electron irradiation for 30 min without additional heating in a magnetic field of 1.7 T (sample C2) and without magnetic field (sample A1). The curves of the tritium fractional release have been calculated for the following values of the initial total tritium activity for 1 cm^2 of the plasma-facing surface, MBq·cm^{-2}: A1 – 2.768; C2 – 1.119. The total charge of the current collected with the probe during the irradiation, mC: A1 – 2.09; C2 – 1.99.

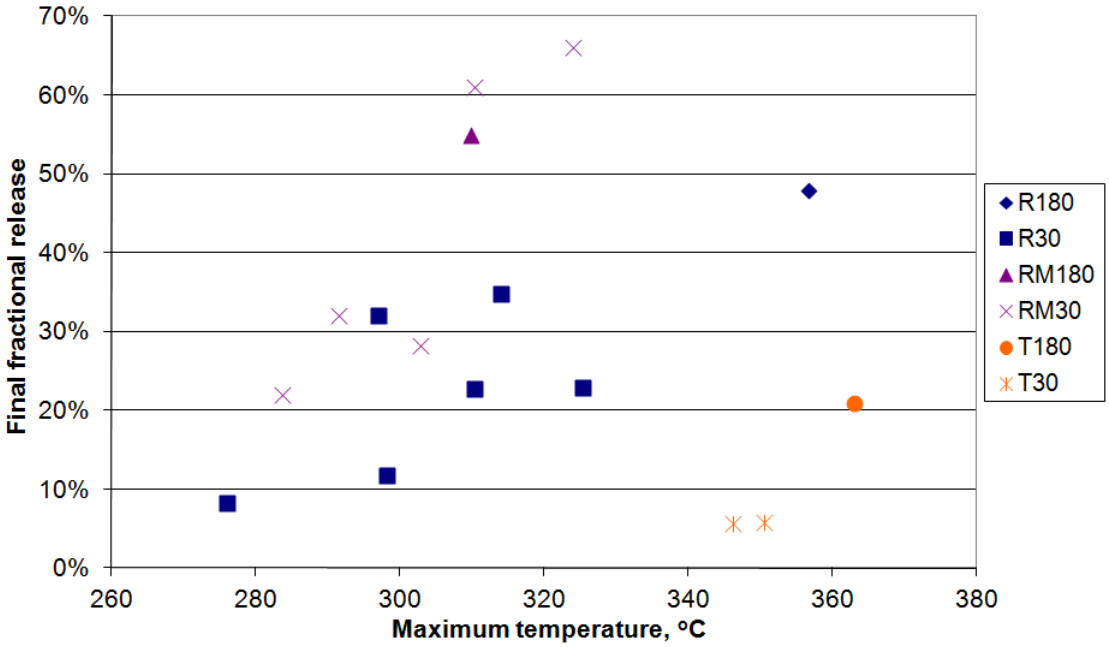

Fig. 4.1.20. Final values of the tritium fractional release as a function of the maximum temperature at annealing. Explanation of the legend: R180 and R30 – the 5 MeV fast-electron irradiation for 180 and 30 min respectively without magnetic field; RM180 and RM30 – the 5 MeV fast-electron irradiation for 180 and 30 min respectively in a magnetic field of 1.7 T; T180 and T30 – only thermal treatment for 180 and 30 min respectively without electron irradiation and without magnetic field.

4.1.4. Overall comparison of the experiment results on tritium release under action of temperature, radiation and magnetic field separately or simultaneously

The oblong samples were dissimilar not only by their initial total tritium activity, which was in the range of 0.5-3.5 MBq·cm^{-2} (Fig. 4.1.1b), but also by their tritium fractional release under the similar conditions. This dissimilarity of the samples limits the ability to draw quantitative conclusions about the magnetic field effect on the tritium release.

The degrees of detritiation achieved in the annealing process are summarized in Fig. 4.1.20 as a function of the maximum temperatures of the samples. The highest degrees of detritiation of 55-66% were achieved only in a magnetic field of 1.7 T. The medium degrees of detritiation of 22-32% were achieved with the electron irradiation in a magnetic field of 1.7 T in most cases at lower maximum temperatures of the samples than those with the electron irradiation without magnetic field or with simple heating without electron irradiation. Therefore, a trend that magnetic field of 1.7 T had a facilitating effect on the tritium release may be concluded from the experimental results.

Regarding the choice of the time of the electron irradiation of 30 min in comparison with 180 min, we may conclude from the tritium release curves that the fractional release rate diminished significantly by the end of the 30 min electron irradiation time in the case of samples 2, 4, 5 and A2, but the fractional release rate remained high by the end of the 30 min electron irradiation time in the case of samples 3, C1, C2, C4, C5, A1, A3-A6. Therefore, we may suggest that prolongation of the electron irradiation would have considerably increased the degree of detritiation of samples 3, C1, C2, C4, C5, A1, A3-A6

4.1.5. Tritium distribution in a tile of MkII Septum Replace Plate (SRP) divertor

Distribution of tritium has been analyzed in the selected tiles of the JET MkII Septum Replace Plate (SRP) divertor, campaign 2001-2004. Samples of tile 14ING3B (Fig. 4.21) was analyzed and analysis of tile 14BWG4B continued for realization the tasks.

Analysis of surface activity of tritium once more confirm the fact that main part of tritium is accumulated in a deposited layer and substantial difference are between the surface and bulk activity and the last slicve at a rear side. Migration of tritium into the bulk of a tile is expected at high temperatures as is clearly demonstrated in the results from the sloping part where the tritium mass activity of the bulk was found to be about an order higher that in other parts of the tile.

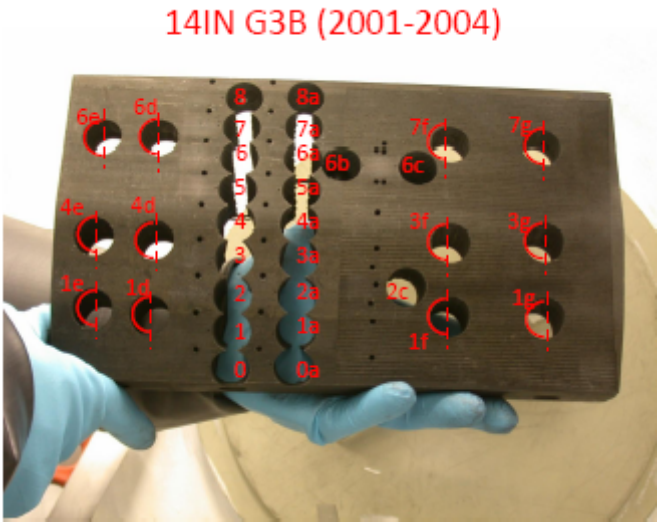

Fig. 4.1.21. Positions of analyzed cylinders of tile 14ING3B, cylinders “e” – without treatment, not detriated and cylinders “f” laser cleaned.

Laboratory analyzed slices cut from both type of cylinders –from cylinders “e” without cleaning, non-detritiated samples and from laser cleaned slices from“f” cylinders. Amount of tritium on plasma facing surface slices, in the bulk and in the back side slices are shown in Figs 4.1.22. - 4.1.23.

The larger part of tritium is concentrated in the first slices A1 (1 mm) for all analyzed cylinders. In the next slice the tritium amount sharply decreases and stayed less or more uniform in the middle of tile and then once more sharply increases in the last slice of the back side.

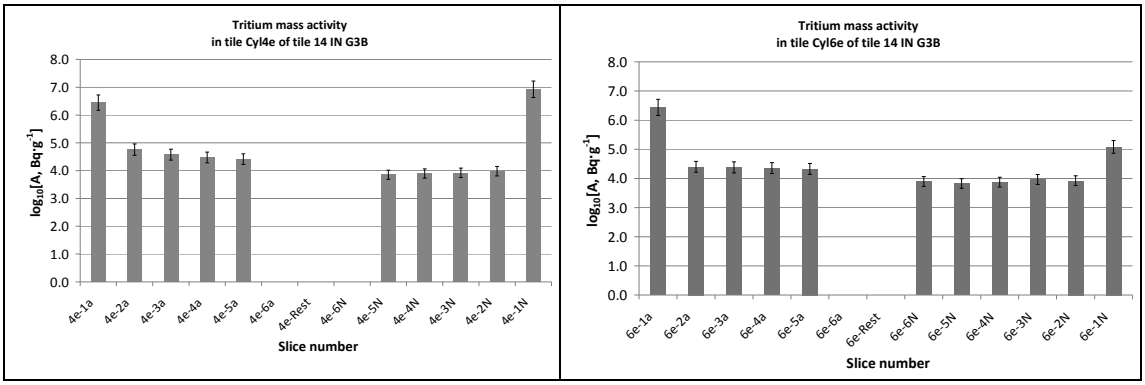

Fig. 4.1.22. Distribution of tritium in non detritiated cylinders Cyl4e and Cyl 6e.

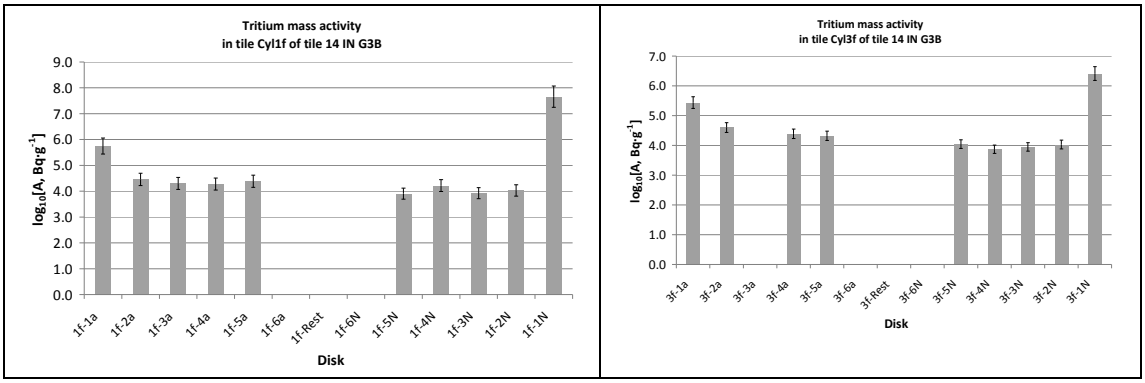

Fig. 4.1.23 Distribution of tritium in laser cleaned cylinders Cyl1f and Cyl 3f

Obtained results show that an effect of laser cleaning could be observed on the first slice, but as analysis was realized with full combustion technique and in this case the thickness of a slice is 1 mm for analysis, to give precious numerical estimation of detritiation degree is difficult, substantially thin slice is necessary to prepare. Additional analyses are necessary in order to explain the large amount of tritium in the last slice of all cylinders.

Conclusions

1. A trend that magnetic field of 1.7 T had a facilitating effect on the tritium release may be concluded from the experimental results.
2. Distribution of tritium in the JET divertor MkII SRP tile show that the largest amount of tritium is accumulated in plasma facing part and in areas at the back side.

4.2. Tritium release from neutron irradiated beryllium pebbles

F4E-2009-GRT-030-A3

Principal investigator: G. Kizane
Staff members:A. Vitins, V. Zubkovs, V. Kinerte, G.Ivanov, O. Pushkova, A. Matiko, A. Matiss

Beryllium pebbles will be used as a neutron multiplier in a solid tritium breeding blanket for fusion reactors. Tritium inventory in beryllium as a result of neutron-induced transmutations is a significant safety and technological issue for the operation of the breeding blanket.
In order to estimate behaviour of beryllium pebbles under exploitation conditions relevant to the ITER and DEMO, the HIDOBE-1 (**Hi**gh **Do**se Irradiated **Be**ryllium) experiment had been performed in the frame of the European Programme for development of the helium cooled pebble bed (HCPB).

The aim of HIDOBE irradiation experiment is to investigate accumulation of tritium, to test thermo-mechanical properties of pebble bed units, to understand tritium release process in presence of high helium concentration up to 3000 appm or 18 dpa. The irradiation had been realized in the High Flux Reactor HFR in Petten (the Netherlands).

Tritium is localised in beryllium in forms of the gas T_2, radicals T^o and ions T^+. In order to determine the abundance ratios of chemical forms, the method of beryllium dissolution with and without presence of chemical scavengers has been used. The main chemical form of the tritium accumulated in beryllium pebbles is molecular T_2. Gaseous tritium could be trapped in a technological void at pebble centre and in the pores, located in the bulk of pebbles. Pebbles of a 0.5 and 1 mm diameter (2001 and 2003 production years) have been analysed and difference in tritium distribution has been observed. Tritium programmed temperature desorption spectra have been obtained, and tritium chemical forms were determined.

4.2.1. Initial chemical forms of accumulated tritium

Be pebbles as neutron multiplier will be under action of a high temperature, neutron flux and high magnetic field. The range of temperature at the operating conditions of the HCPB of different designs is given different - up to 920 K (647 ^oC), 700-1050 K **(**427-777^oC**)** or up to 1170 K (897^oC), but the latest information is that the maximum interface temperature of 823K (550 ^{o} C) is chosen. Tritium release and retention is dependent on beryllium properties (structure, impurities, grain size, diameter of a pebble, porosity etc.), on irradiation conditions (neutron flux, temperature, content of purge gas etc.), on chemical impurities.

In order to understand and explain tritium retention and release process from neutron irradiated beryllium pebbles, it is necessary to know initial chemical forms of accumulated tritium. In the year 2011, the chemical forms of HIDOBE beryllium pebbles have been determined. Tritium accumulated in the HIDOBE-I beryllium pebbles has been localized in forms of the gas T_2, radicals T^o and ions T^+. In order to determine the total tritium mass activity and the abundance ratios of chemical forms of tritium, dissolution method (Fig. 4.2.1) based on a selective reaction of chemically active particles with scavengers was used.
Two different dissolution systems were used for analysis of a pebble:

- 2 mol/L H_2SO_4.

The dissolution of a separate pebble in pure acid transfer the T_2 and T^0 localized in the Be pebbles as T_2+HT into a gas phase.
T^+ localized in a Be pebble remains in the solution.

- 2 mol/L H_2SO_4 with 0.5-1 mol/L $Na_2Cr_2O_7$.

The dissolution of a pebble in acidic solution in a presence of $Na_2Cr_2O_7$ gives additional data to determine the chemical forms of tritium T^0 and T_2 separately.
In order to decrease dissolution rate and to prevent release of large amount of tritium at dissolution processes, dissolution in only 0.5 M sulfuric acid was used. Experiments with non-irradiated beryllium pebbles were performed in order to estimate the time of dissolution.
The rate of tritium release was measured continuously with a tritium monitor TEM 2100A with a detector DDH 32. Tritium T^+ localized in the solution was analyzed by liquid scintillation method. Each pebble before weighting was washed and dried. Distillation of the dissolution solution was performed before LSM analysis of amount of tritium, in order to prevent influence of radioactive isotope ^{60}Co . The contents of T^0, T_2 and T^+ (Bq g^{-1}) in the sample were calculated from the tritium activities in a gas phase and in the solution.

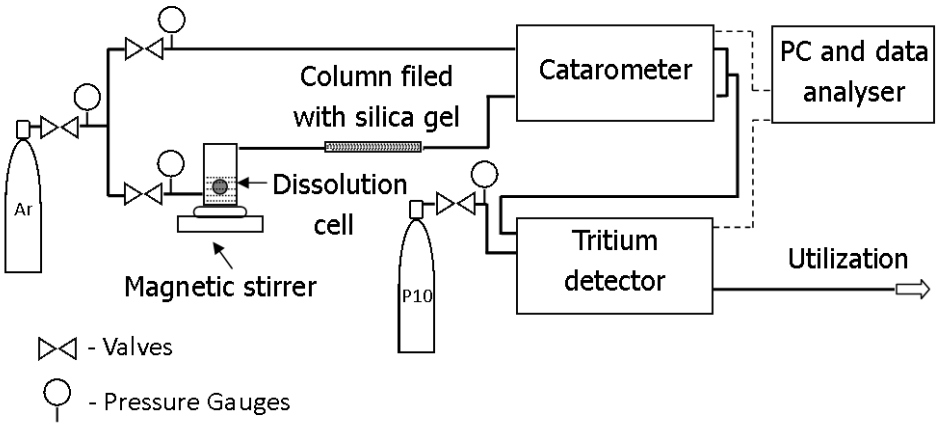

Fig. 4.2.1.Dissolution system and beryllium pebble placed on surface of magnetic stirrer in the dissolution cell.

Mass activity of tritium in the pebble correlates with irradiation temperature, if we compare amount of accumulated tritium at the highest irradiation temperature - 750 ^{o}C with tritium amount accumulated at 425, 550 and 650 ^{o}C, but at the same time at temperatures 425, 550 and 650 ^{o}C the activities of tritium are similar, influence of irradiation temperature isn't substantial.

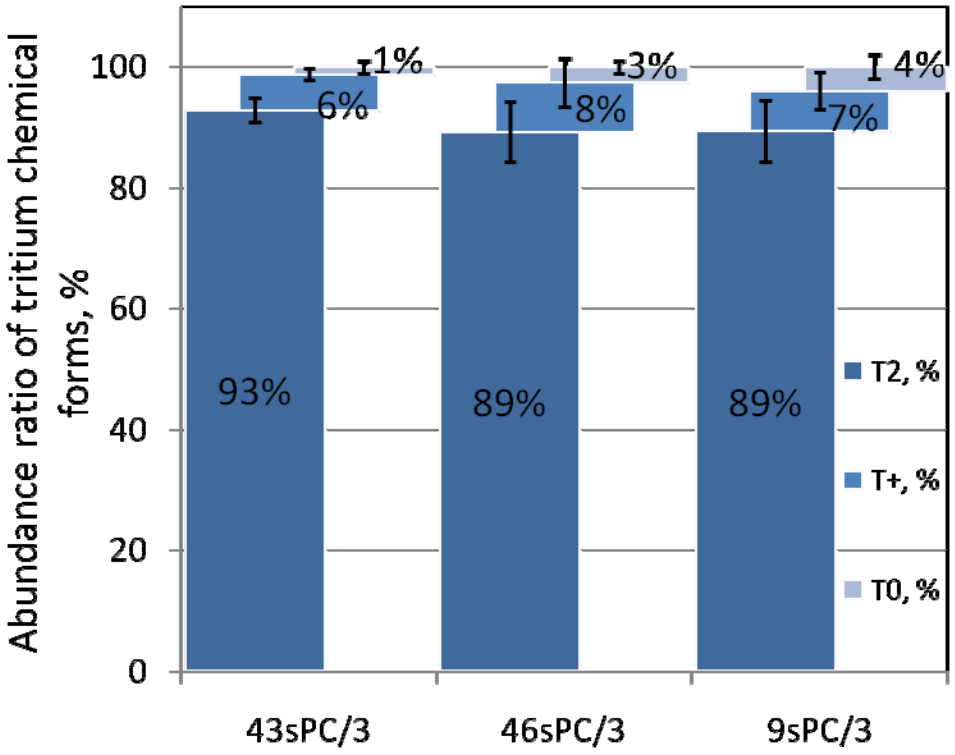

Fig.4.2.2. Chemical forms of tritium in the pebbles of the three analyzed series are given as bar graphs.

Abundance ratio of tritium chemical forms might be assumed to be similar. Only slight differences that do not exceed confidence level are observed for the pebbles synthesized in the year 2003. Higher amount of molecular tritium was observed in pebbles produced by improved method in 2003.

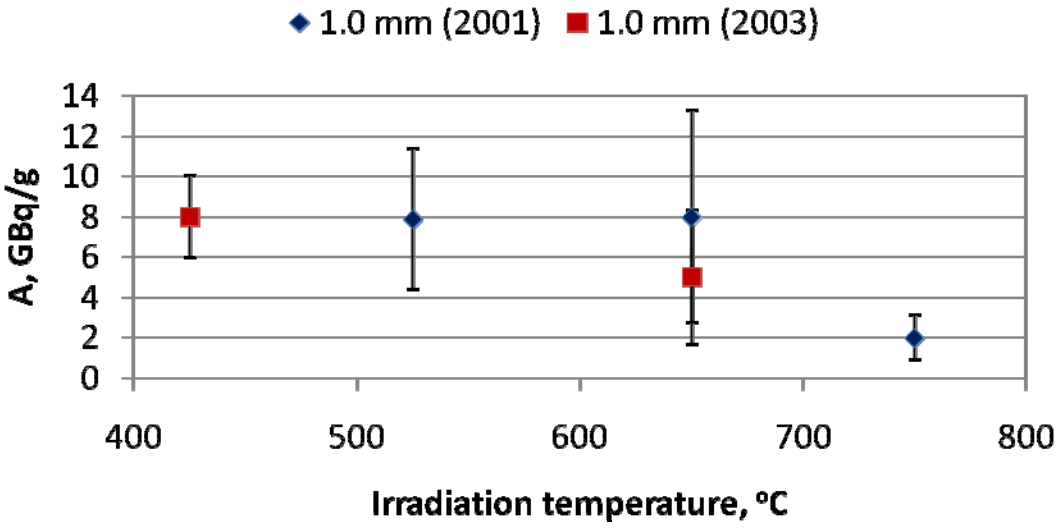

Fig.4.2.3. Mass activity of tritium in the HIDOBE–01 pebbles as a function of the irradiation temperature in the HFR.

Analysis of chemical forms for 1 mm and 0.5 mm diameter pebbles has been realized for batches shown in Fig. 2 and Table 1.

Table 1.

Activity of tritium in HIDOBE-01 pebbles.

Sample	**Irradiation T, °C**	**Coding**	**Number of dissolute pebbles**	**Average activity, GBq/g**	**Standard deviation**	**Average activity, GBq/g**
1.0 mm (2001)	650	10sPC/3	2	8.00	0.59	8±5
1.0 mm (2001)	750	9sPC/3	6	1.75	1,05	2±1
1.0 mm (2003)	650	6sPC/3	3	5.28	1.34	5±3
0.5 mm	750	1sPC/3	2	0.38	0.32	1±3

Distribution of tritium in a pebble also depends on irradiation temperature. At 750 °C the distribution of tritium is regular, but at other temperatures tritium is concentrated in a centre of pebble.

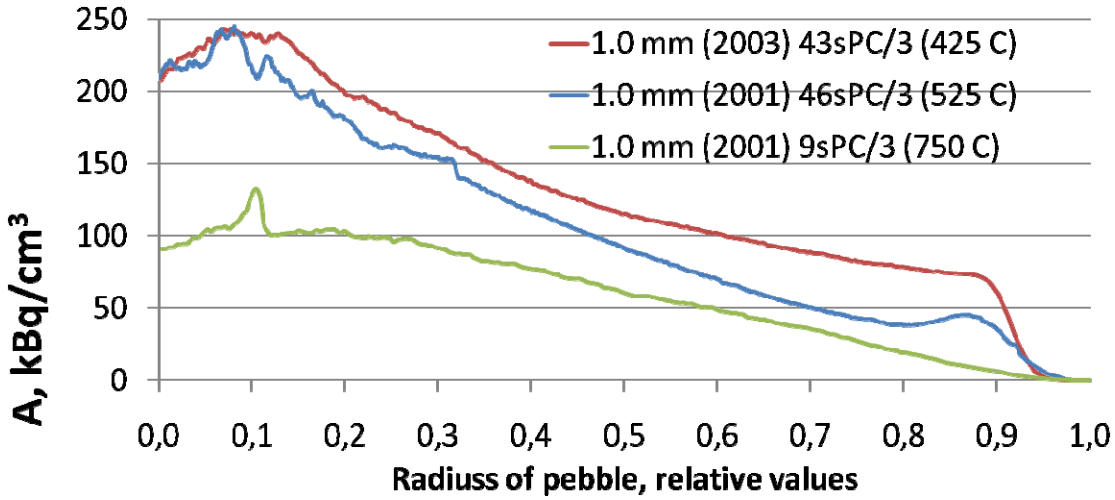

Fig. 4.2.4. Distribution of tritium in the pebbles.

Tritium accumulated in the HIDOBE-I beryllium pebbles has been localized in forms of the gas T_2 and T^o and ions T^+. The main chemical from of the tritium accumulated in the HIDOBE-I beryllium pebbles is molecular tritium T_2- 94±2 %, atomic tritium T^o only 2± 2% and tritium in ionic form 6±1 %.

4.2.2. Tritium release under action of temperature

Post irradiation tritium room temperature to 1310 K and anneals at a constant temperature of 1 h on the beryllium pebbles were performed. One Be pebble was investigated in each tritium release experiment. The tritium release was performed in a continuous flow of the purge gas He + 0.1% H_2 of the rate 14-16 L/h. Histograms of the tritium release rate and curves of the tritium sum release from HIDOBE beryllium pebbles are given in Figs. 4.2.5-4.2.7. Tritium release begins for all of investigated HIDOBE-I beryllium pebbles at temperatures 850-900 °C and after 900 °C starts fast tritium release process. Amount of accumulated and retained tritium is very dissimilar for one batch; but for different batches it differs even 22-58 times each from another pebble (Fig.4.2.5-and Fig. 4.2.6).

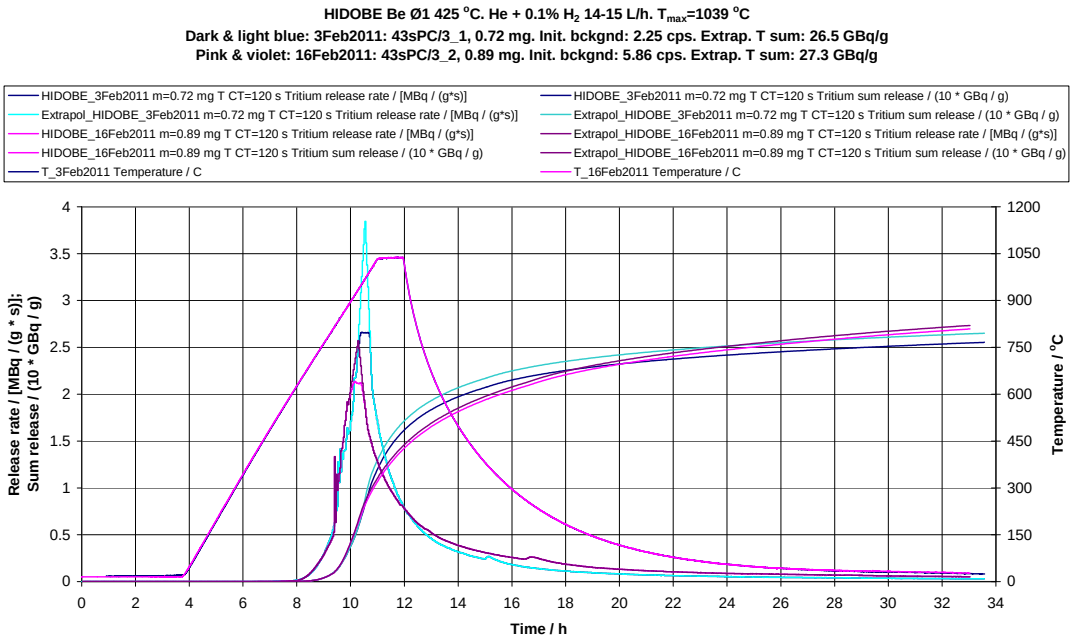

Fig. 2.2.5. Tritium release rate and tritium sum release from high level activity HIDOBE-01 beryllium pebbles irradiated at 425 °C, heated at the given temperature. Curves dark blue-light blue – the HIDOBE Be pebble of 0.72 mg, the tritium sum release 26.5 GBq/g. Curves pink-violet – the HIDOBE Be pebble of 0.89 mg, the tritium sum release 27.3 GBq/g.

High level of the tritium activity retained in the samples of Fig. 4.26 is understandable – it is related to low irradiation temperature in the HFR - 425 °C. In reality significant tritium release starts at temperatures higher than 850 -900 °C. It should be noted that the HIDOBE Be pebbles irradiated at 425 °C had considerably higher tritium release rates even 20 h after the end of the temperature program, after cooling down below 60 °C (Fig. 4.26) than those of the HIDOBE Be pebbles irradiated at 750 °C (Fig. 4.27).

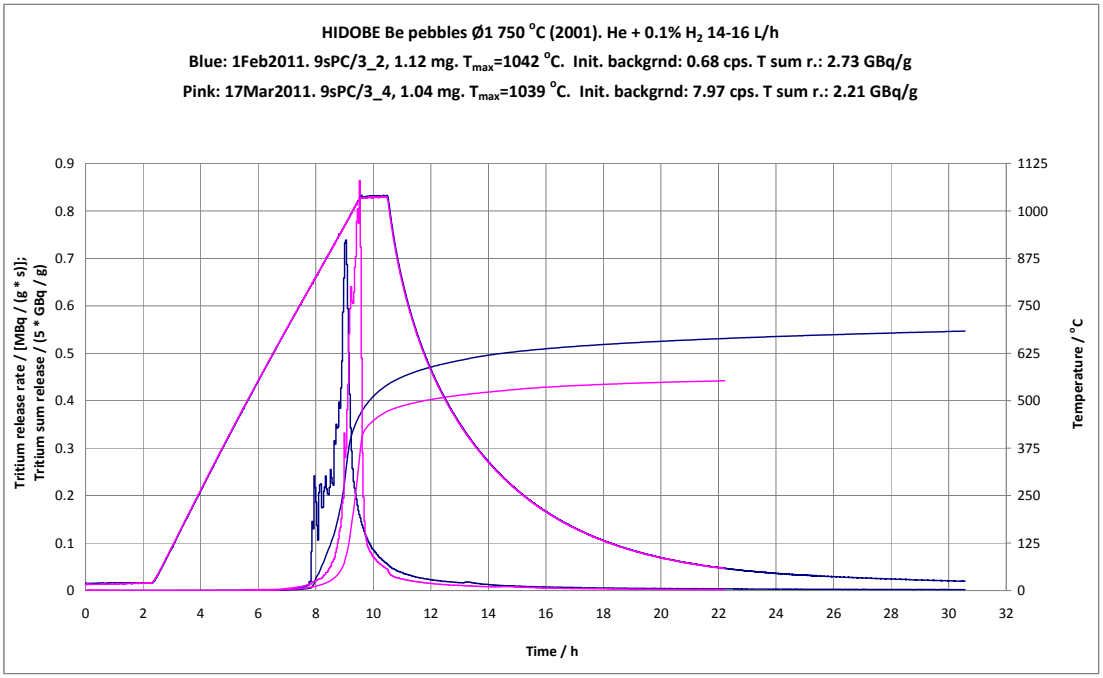

Fig.4.2.6. Tritium release rate and tritium sum release from the HIDOBE-01 beryllium pebbles irradiated at 750 ^{o}C, having lower level tritium activity heated at the given temperature. The dark blue curves – the HIDOBE Be pebble of 1.12 mg, the tritium sum release 2.73 GBq/g. The pink curves– the HIDOBE Be pebble of 1.04 mg, the tritium sum release 2.21 GBq/g.

Tritium release from pebbles at 1039 °C temperature for 1 h long time with lower tritium activity (1-3 GBq) goes more effective. Residual tritium had been determined by dissolution method and was only some kBq. Tritium release even from three beryllium pebbles of one batch is very dissimilar. Fig. 4.2.7 shows tritium release histograms from three pebbles of the same batch. 9SPc/3.

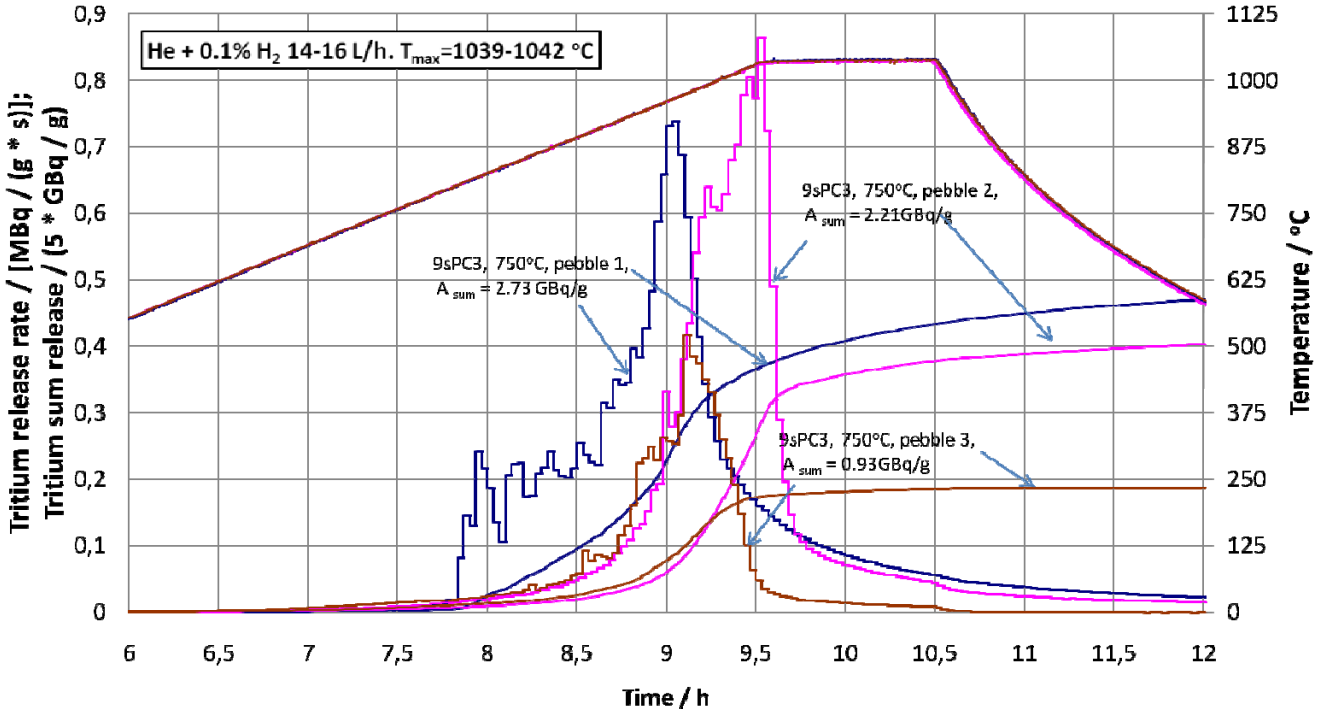

Fig.4.7. Tritium release rate and tritium sum release from the HIDOBE-01 beryllium pebbles having lower level tritium activity heated at the given temperature. The blue curves – the HIDOBE Be pebble of 1.12 mg having the tritium sum release 2.73 GBq/g. The pink curves – the HIDOBE Be pebble of 1.04 mg, the tritium sum release 2.21 GBq/g. The brown curves – the HIDOBE pebble the tritium sum release 0.93 GBq/g.

Conclusions

- Tritium content in irradiated pebbles depends on irradiation temperature: at lower temperatures more tritium is left in the pebble.

- Most of the tritium is accumulated as a molecular T_2 (89-93%), whereas chemically bonded to oxygen T^+ is 5-10% of tritium. Atomic tritium T^o does not exceed 4-7%% of the total content.
- Tritium thermo-desorption process is considerably different even within one type of pebbles. For estimation of desorption mechanisms and reasons for such differences more measurements are needed.
- Investigated pebbles were different by their mass (0.67-1.34 mg), by their initial total tritium activity and by their tritium fractional release under the given conditions

Collaboration

1. KIT, Germany –Dr. A. Möslang, Dr. V. Chakin –
    - on the investigations of the irradiated Be HIDOBE-I pebbles;
    - in the frame of EFDA Goal Oriented Training Programme "EUROBREED"
2. KIT, Germany –Dr. R. Knitter – common investigations of lithium orthosilicate pebbles blanket breeder materials, 1 joint publication prepared;
3. NRG, the Netherlands – Dr. L. Magielsen, MSc. S.van Til- in the frame of the PIE experiments on HIDOBE-I beryllium pebbles;
4. TEKES, Finland – Dr. Jari Likonen, on analysis of tritium in carbon based samples.
5. MDeC, Romania – Dr. C.atalin Stansion, on analysis of tritium in carbon based samples.
6. Tarty University – Dr. Madis Kiisk -on analysis of tritium in carbon based samples.

5. STAFF MOBILITY ACTIONS

5.1. STAFF MOBILITY VISITS

Gunta Kizane took part in:

- 5th Progress Meeting Breeder Blanket Be pebbles, Madrid, 22-25Mai, 2011,
- Progress Meeting HIDOBE-1, 8-19 Mai, Petten
- 6th Progress Meeting on the GOTP "EUROBREED", 13-18 Nov, 2011, Karlsruhe
- General Monitoring Meeting to present the status of work under tasks " JW9-FT-3.46", JW10-FT-3.62, JW11-FT-1.19" and present an explanation of the background, purpose and objectives of the task JW11-FT-1.20 at the Kick-off Technical meeting, 23–27Dec, 2011, the JET, Culham Science Centre, Abingdon, UK. Oral presentation

Elina Pajuste	took part in: • ENYGF-11 –forum of young generation, Praha, 17 - 21Mai2011 • 5th Progress Meeting on the GOTP "EUROBREED", Madrid, 22-25Mai, 2011, • 6th Progress Meeting on the GOTP "EUROBREED", Karlsruhe, 22-25Nov, 2011,
Olgerts Dumbrajs	IPP Garching, 1 May – 30 May, 2011 IPP Garching, 1 June – 30 June, 2011
Jurijs Zhukovskis	KIT Karlsruhe, 29 May – 12 June, 2011 KIT Karlsruhe, 5 October – 20 October, 2011
Olgerts Lielausis	IPP Garching, 12 April -16 April, 2011 IPP Garching, 28 July – 30 July, 2011 IPP Garching, 4 October – 6 October, 2011 IPP Garching, 26 October – 29 October, 2011

6. OTHER ACTIVITIES

6.1. Conferences, Workshops and Meetings

Results of fusion research were presented at the conferences:

1. The 27th Scientific Conference of Institute of Solid State Physics. University of Latvia, Riga, February 14-16, 2011.
2. International Baltic Sea Region Conference "Functional Materials and Nanotechnologies 2011" (FM&NT-2011) Riga, April 2011. – Institute of Solid State Physics, University of Latvia.
3. 69th conference of University of Latvia, section of Analytical and physical chemistry, Riga, Latvia February 18, 2011.
4. *European Nuclear Young generation Forum 2011* (ENYGF 2011), Czech Technical University: Prague, Czech Republic, May 17 -22, 2011.

5. 8th International workshop „Strong microwaves and terahertz waves. Sources and applications“, Nizhny Novgorod , Russsia, July 6-16, 2011.
6. Telephone-conference I Semi annual monitoring meeting - JET Fusion Technology on the tasks JW9-FT-3.46, JW10-FT-3.62 , JW11-FT=-1.19 on the 5th June 2011.

7. PUBLICATIONS 2011

7.1. FUSION PHYSICS AND PLASMA ENGINEERING

7.1.1. Publications in scientific journals

1. R.B.Gomes, C.Silva, H.Fernandes, P.Duarte, I.Nedzelskiy, O.Lielausis, A.Klykin, E. Platacis - “ ISSTOK tokamak plasmas influence on a liquid gallium jet dynamic behavior”, Journal of nuclear materials 415(2011) S989-S992
2.O. Lielausis, A. Klykin, E. Platacis, A. Mikelsons, R.B. Gomes, H. Fernandes, C. Silva “Stability of liquid metal jet in the context of fusion applications” Proc. Int. Conf. Fundamental and applied MHD, Pamir 2011 V.1, p.257-260.- Borgo-Corsica-France September 5-9, 2011.
3. O. Dumbrajs, „Influence of possible reflections on the operation of European ITER gyrotrons” J. Infrared Milli. Terahz. Waves **31**, 892 (2010).
4. O. Dumbrajs, T. Idehara, and S. Sabchevski, “Design of an optimized resonant cavity for a compact sub-Terahertz gyrotron” J. Infrared Milli. Terahz. Waves **31**, 1115 (2010).
5. A. Reinfelds, O. Dumbrajs, H. Kalis, J. Cepitis, and D. Constantinescu, „Numerical experiments with single mode gyrotron equations” Mathematical Modelling and Analysis **17**, 251 (2012).
6. D. Constantinescu, O. Dumbrajs, V. Igochine, K. Lackner, R. Meyer-Spasche, and H. Zohm, “A low-dimensional model system for quasi-periodic plasma perturbations” Phys. Plasmas **18**, 062307 (2011).
7. Erzhong Li, Liqun Hu, V. Igochine, O. Dumbrajs, and Kaiyun Chen, „Understanding complex magnetohydrodynamic activities associated with a relaxation in HT-7 tokamak” Plasma Phys. Control. Fusion **53**, 085019 (2011).
8. A. Gopejenko, Yu.F. Zhukovskii, P.V. Vladimirov, E.A. Kotomin, and A. Möslang, *Modeling of yttrium, oxygen atoms and vacancies in γ-iron lattice*. - J. Nucl. Mater., **2011**, **416**, p. 40-44.

7.1.2. Conference articles

1. A. Gopejenko, Yu.F. Zhukovskii, P.V. Vladimirov, E.A. Kotomin, and A. Möslang, „Ab initio calculations of binding energies between defects in fcc Fe lattice”. 27th ISSP Conference (Riga, Latvia, February, 2011)Abstracts: p. 6

2. A. Gopejenko, Yu.F. Zhukovskii, P.V. Vladimirov, E.A. Kotomin, and A. Möslang, “Ab initio calculations of pair-wise interactions between defects for ODS steels”. International conference "Functional materials and nanotechnologies" FM&NT-2011 (Riga, Latvia, April, 2011). Abstracts: p. 165.

3. A. Gopejenko, Yu.F. Zhukovskii, P.V. Vladimirov, E.A. Kotomin, and A. Möslang, *"Interactions between Y and O impurity atoms as well as Fe vacancies in*

iron lattice: Ab initio modeling". 9th International Conference "Information Technologies and Management",IT&M'2011(Riga, Latvia, April, 2010). Abstr.: p. 46.

4. A. Gopejenko, Yu.F. Zhukovskii, P.V. Vladimirov, V.A. Borodin, E. A. Kotomin, and A. Möslang, *"Modelling of interactions between Y, O and vacancy clusters in fcc Fe lattice"*. Spring European Materials Research Society (E-MRS) Meeting (Nice, France, May, 2011). Abstracts: VP-7.

5. Yu.A. Mastrikov, Yu.F. Zhukovskii, E.A. Kotomin, P.V. Vladimirov, and A. Möslang, "Models of point defects in *bcc*-Fe lattice for simulation of ODS nanocluster". Spring EFDA Monitory Meeting of European Fusion Development Agreement (Frascati, Italy, June, 2011).

6. A. Gopejenko, Yu.F. Zhukovskii, P.V. Vladimirov, E.A. Kotomin, and A. Möslang, "Interaction of O and Y impurity atoms as well as Fe lattice: Ab initio modeling". NATO Advanced Research Workshop "Nanomaterials and Nanodevices for Ecological Security" (Jurmala, Latvia, June, 2011). Abstracts: PB06

7. Yu.A. Mastrikov, P.V. Vladimirov, V.A. Borodin, Yu.F. Zhukovskii, E.A. Kotomin, and A. Möslang "*Large-scale DFT calculations on Fe vacancies and Y impurity atoms in bcc-iron supercells".* Fall EFDA Monitory Meeting of European Fusion Development Agreement (Garching, Germany, November, 2011).

7.2. FUSION TECHNOLOGY

7.2.1. Publications in scientific journals

1. 1. E. Pajuste,A. Vitins,G. Kizane,V. Zubkovs and P. Birjukovs Tritium distribution and chemical forms in the irradiated beryllium pebbles before and after thermoannealing. Fusion Engineering and Design. October 2011. 86(9-11), 2125-2128.

2. E. Pajuste, G. Kizane, J.P. Coad, A. Vitins, A. Kirillova, M. Halitovs and JET-EFDA Contributors Structural changes and distribution of accumulated tritium in the carbon based JET tiles**.** *Journal of Nuclear Materials*, August 2011. 415 (1), S765-S768.

3. A. Vītiņš, V. Zubkovs, G. Ķizāne, E. Pajuste and V. Kinerte Tritium release characteristics of neutron-irradiated reference beryllium pebbles for the helium cooled pebble bed (HCPB) blanket. *Fusion Science and Technology*, October 2011. *60*(3), 1143-1146.

Submitted:

1. A. Zarins, A. Supe, G. Kizane, R. Knitter, L. Baumane Accumulation of radiation defects and products of radiolysis in slightly overstoichiometric lithium orthosilicate pebbles *Journal of Nuclear Materials,* submitted on 10th July, 2011

2. Aigars Vītiņš , Gunta Ķizāne, Andris Matīss, Elīna Pajuste, Vitālijs Zubkovs Tritium Release from the Pebble-Bed Assemblies Neutron-Irradiated Beryllium Pebbles under Action of Temperature. *Journal of Nuclear Materials,* submitted on 5th October, 2011.

7.2.2. Conference articles

Proceedings published

1. A. Zarins, G. Kizane, B. Lescinskis, L. Avotina, A. Berzins, I. Steins. Changes of stehiometric and nonstehiometric nanopowders of lithium orthosilicate under thermal treatment and action of moisture. In International *Conference of Young Scientists on Energy Issues 2011* (CYSENI 2011), May 26-27, Kaunas, Lithuania. Conference proceedings, ISSN 1822-7554, VII-334-340, available on-line at www.cyseni.com.

2. M. Halitovs, G. Kizane, A. Vitins, E. Pajuste, L. Avotina Depth profiles of tritium accumulated in carbon fibre composite divertor materials of JET fusion reactor. CYSENI 2011, In *Conference of Young Scientists on Energy Issues 2011* (CYSENI 2011), ISSN 1822-7554, 2011, X-442-448 available on-line at www.cyseni.com.

3. V. Zubkovs, E. Pajuste, G. Kizane, A. Vitins, A. Matiss, Tritium localization in the bulk of neutron irradiated beryllium pebbles. CYSENI 2011, In *Conference of Young Scientists on Energy Issues 2011* (CYSENI 2011), ISSN 1822-7554, 2011, X-538-544 available on-line at www.cyseni.com.

International conferences

1. Aigars Vītiņš , Gunta Ķizāne, Andris Matīss, Elīna Pajuste, Vitālijs Zubkovs Tritium Release from the Pebble-Bed Assemblies Neutron-Irradiated Beryllium Pebbles under Action of Temperature. In. 15th International Conference on Fusion Reactor Materials (ICFRM-15), Charleston, South Carolina, USA, October 16-22, 2011, p. 15-231

2. Gunta Ķizāne, Aigars Vītiņš, Elīna Pajuste, Mihails Haļitovs, Arturs Zariņš, Vitālijs Zubkovs, Sanders van Tils Tritija uzkrāšanās kodolsintēzes reaktoru materiālos. In. Apvienotais pasaules latviešu zinātnieku III kongress, 24.-27. Oktobris, 2011, Rīga, p. 110.

3. V. Zubkovs, O. Paskova, A. Matiko, G. Kizane, E. Pajuste. Issues Related to Tritium Inventory in the neutron Irradiated Beryllium Pebbles. In *13-th International Conference-School „Advanced Materials and Technologies*", August 27 - 31 2011, Palanga, Lithuania, p.144.

4. L. Avotina, M. Halitovs. Microcrystalline Structure of Divertor Materials Researched by X-ray Diffractometry and Raman Spectroscopy. In *13-th International Conference-School „Advanced Materials and Technologies"*, August 27 – 31, 2011, Palanga, Lithuania, p.149.

Local conferences

1. A. Vītiņš, G. Ķizāne, A. Matīss, E. Pajuste, V. Zubkovs, Tritium release from neutron-irradiated beryllium pebbles under action of temperature. In *Abstracts of the 27th Scientific Conference of the Institute of Solid State Physics of the University of Latvia Dedicated to the Fiftieth Anniversaries of the Laboratory of*

Problems of Semiconductor Physics of the University of Latvia and the Nuclear Reactor at Salaspils, February 14-16, 2011. A. Krūmiņš, Editor. Institute of Solid State Physics: Riga, Latvia. P. 9.

2. V. Zubkovs, A. Vītiņš, G. Ķizāne, E. Pajuste, A. Matīss, Comparison of tritium distribution in different neutron irradiated beryllium pebbles. In *Abstracts of the 27th Scientific Conference of the Institute of Solid State Physics of the University of Latvia Dedicated to the Fiftieth Anniversaries of the Laboratory of Problems of Semiconductor Physics of the University of Latvia and the Nuclear Reactor at Salaspils*, February 14-16, 2011. A. Krūmiņš, Editor. Institute of Solid State Physics: Riga, Latvia. P. 75.

3. M. Haļitovs, G. Ķizāne, L. Avotiņa, E. Pajuste, Distribution of tritium in poloidal and toroidal dirrection of tiles of the MKII-SRP divertor. In *27th Scientific conference of Institute of Solid State Physics*, February 14-16, 2011, Institute of Solid State Physics: Riga, Latvia. p. 77.

4. A. Zariņš, G. Ķizāne, B. Leščinskis, L. Avotiņa, A. Bērziņš, I. Šteins, Changes of nanopowders of lithium orthosilicate under action of moisture. In *27th Scientific conference of Institute of Solid State Physics*, February 14-16, 2011, Institute of Solid